CONF-781065--1

AN OVERVIEW OF EXPERIMENTAL RESULTS OBTAINED UNDER THE PRESTRESSED CONCRETE NUCLEAR PRESSURE VESSEL DEVELOPMENT PROGRAM AT THE OAK RIDGE NATIONAL LABORATORY*

D. J. Naus
Oak Ridge National Laboratory
Oak Ridge, Tennessee 37830

ABSTRACT

Under the Prestressed Concrete Nuclear Pressure Vessel Development Program at the Oak Ridge National Laboratory, various aspects of Prestressed Concrete Pressure Vessels (PCPVs) are investigated and evaluated with respect to reliability, structural performance, constructability, and economy. Based upon identified needs, analytical and experimental investigations are conducted. Areas of interest include finite-element analysis development, materials and structural behavior tests, instrumentation evaluation and development, and structural model tests. Studies have been recently completed in the following areas: concrete embedment instrumentation systems for PCPVs, grouted-nongrouted prestressing systems, acoustic emission as a technique for structural integrity monitoring, and model tests of steam-generator cavity closure plugs for a Gas-Cooled Fast Reactor (GCFR). An overview of results will be presented.

Under the instrumentation evaluation task, 13 types of commercially available concrete embedment strain meters were evaluated with respect to general performance, performance in a simulated PCRV environment, and performance under extreme operating conditions. General conclusions obtained were that (1) meter selection should be based on specific applications, (2) meter calibration factors should be determined for each application, (3) improved materials and sealing techniques are needed, and (4) other promising measurement techniques should be evaluated.

Grouted and nongrouted posttensioning prestressing systems were investigated under the structural models task. The investigation was divided into: relative performance of grouted and nongrouted systems, an evaluation of selected new materials for PCPV applications, and a limited corrosion study to demonstrate the corrosion-inhibiting capability of grout. Results indicate that: grouted tendon beam elements provide improved crack control, improved ultimate load capacity in flexure, and anchorage

*Research sponsored by the Nuclear Power Development Division, U.S. Department of Energy under contract W-7405-eng-26 with the Union Carbide Corporation.

conservatism; the polymer-silica cement and fibrous concrete exhibit potential for PCPV application; and grout provides corrosion-inhibiting capability equivalent to commercial organic petrolatum-based products.

Acoustic emission (AE) is being evaluated as a technique for monitoring the structural integrity of pressurized systems. Data have been obtained from monitoring of prestressed concrete beams tested to failure. General results indicate that AE is applicable to prestressed concrete and can be utilized to detect the onset and propagation of flaws, identify prior loading levels, and locate flaws.

Proposed designs of the PCRV steam-generator cavity and central cavity closure plugs for a prototype GCFR are being evaluated using relatively small scale models. To date, two model tests have been conducted for the steam-generator cavity closure. Results indicate that the designs are overly conservative. Parallel analytical studies have shown the need for improved constitutive equations for concrete in order to provide capability for predicting the characteristic punching shear-type failures of the models.

INTRODUCTION

Under the Prestressed Concrete Nuclear Pressure Development Program at the Oak Ridge National Laboratory, various aspects of Prestressed Concrete Pressure Vessels (PCPVs) are investigated with respect to reliability, structural performance, constructability, and economy. These investigations are conducted under the High-Temperature Gas-Cooled Reactor (HTGR) Program and the Gas-Cooled Fast Reactor (GCFR) Program. The objectives are to: (1) provide technical support to ongoing PCPV design activities, (2) contribute to the overall technological data base, and (3) provide independent review and evaluations. The basic activities and their interaction for meeting these objectives are shown in Fig. 1.

Specific areas of interest at present include finite-element analysis development, materials and structural behavior tests, instrumentation evaluations and development, and structural model tests. The following provides an overview of both the HTGR and GCFR PCPV activities and a summary of recent experimental results.

HTGR BASE TECHNOLOGY PROGRAM OVERVIEW

The HTGR research and development program consists of generic studies divided into the following nine task areas:

1. Analytical Studies
2. Head Failure Studies
3. Concrete Properties in Nuclear Environment
4. Concrete Creep and Creep Recovery
5. Tendon Investigations
6. Liners and Penetrations
7. Instrumentation Evaluation Studies
8. Concrete Structures Testing
9. Program Management and Miscellaneous Activities

A summary of activities under each of these task areas is presented below. Task areas 7 and 8 will be discussed in more detail under the section on recent experimental results.

A series of analytical studies have been conducted to both demonstrate capability to analyze the complex PCPVs and to provide an independent evaluation of the adequacy of a proposed design. The finite-element method of analysis forms the basis for activities designed to provide more accurate concrete constitutive equations, crack representation, and modeling of steel reinforcement. A concrete constitutive model based on the endochronic theory[1] is being used in conjunction with the ADINA finite element code to provide a more accurate representation of the stress-strain behavior of various concretes, concrete multiaxial stress-strain behavior, and hysteresis loops for repeated loadings.

An extensive experimental and analytical investigation of PCPV head failure has been conducted at the University of Illinois. The overall objective of the studies was to develop and verify an analytical procedure to determine the strength of end slabs of PCPVs. Variables were selected to reflect the geometry of slabs covering the main cavity for the current generation of vessel designs. Included were concrete strength, slab span-to-depth ratio, and penetration size and arrangement. A satisfactory analytical model must be capable of simulating the behavior of the end

slab throughout the entire range of response with automatic differentiation between the various failure mechanisms. Results from a total of 35 vessel pressure tests have shown that the mechanism of failure is a function of the slab span-to-depth ratio and the size and number of penetrations. The presence of penetrations affected the strength of the end slab only in the case of purely shear failure mechanism. A final report on this task is in preparation.

A literature review of the properties of unreinforced concrete in a nuclear environment has been conducted and a topical report published.[2] R2
Present activities are related to the design of a concrete multiaxial testing system capable of measuring concrete properties at both room and elevated temperature.

Creep and creep recovery studies of sealed concrete cylindrical specimens have been conducted at the University of Texas and U.S. Army Corps of Engineers Waterways Experiment Station. Variables in the investigation were aggregate type, curing history, test temperature, and state of stress. These studies have been completed and reports published.[3,4] R3

Reports have been recently published presenting results of two PCPV model tests: (1) thermal cylinder experiment designed to provide information for evaluating the capability of analytical methods to predict stress-strain behavior of the barrel portion of a single-cavity PCPV,[5] R5
and (2) concrete moisture migration experiment to obtain information regarding the nature of moisture movement and rate of moisture loss in a PCPV for thermal crossfalls of 0 and 27°C.[6] R6

Detensioning of the axial prestressing tendons of the PCPV thermal cylinder model revealed a number of the inner-row 7-wire tendons having failed during the extended testing period. The post mortem investigation showed that the failures apparently resulted from stress corrosion cracking in the presence of a unique environment consisting of a combination of free ammonia, moisture, and CO_2 (Ref. 7). R7

A program of experimental studies is under way to: (1) define a reference fracture toughness curve for ferritic components of the HTGR primary pressure boundary, (2) define a temperature indexing procedure for the K_{IR} curve based on standard materials qualifications tests, and (3) obtain a sufficiently large quantity of fracture toughness data so that

a statistically meaningful evaluation of data can be conducted as a tool to help assess the probability for component failure. Materials presently being investigated are ASTM A537 plate and A508 class 1 forging. Weldments and heat-affected zone samples are also being tested.

Another important activity of the generic program is the collection and dissemination of published information on PCPV development. Current activities include the design of a model test for an offset core PCPV, and preparation of a plan for the development of an optimized PCPV.

GCFR PROGRAM OVERVIEW

The PCPV for the Gas-Cooled Fast Reactor (GCFR) is relatively unique with respect to its high operating pressure and the requirement of a large penetration closure to provide access to the core cavity. It is therefore necessary to design, build, and test models of entire PCPVs and the closures for both the steam generator and core cavities. The objectives of the tests are to (1) measure structural response for design and off-design operating conditions, (2) determine plug failure modes, and (3) provide reliable data for verification of analysis methods. Testing has been completed on two relatively small models of proposed designs for the steam-generator cavity closure. Present activities include an analytical parametric study of the core cavity closure and development of a facility for testing larger models.

RECENT EXPERIMENTAL STUDIES UNDER THE HTGR PROGRAM

The following sections will summarize the findings of recent experimental studies conducted under the generic program.

Embedment Instrumentation for PCPVs

Numerous commercial concrete embedment instrumentation systems are available for indicating strains, stresses, loads, and moisture content in PCPVs. An investigation was conducted to determine the relative performance of concrete embedment strain meters. Thirteen types of commercially available strain meters were selected for evaluation. The large

number of different types and brands of strain meters available necessitated that, at least initially, the study restrict itself to meters readily obtainable in the United States. The meters, presented in Table 1, were evaluated with respect to general performance, performance in a simulated PCPV environment, and performance under extreme operating conditions. T1

General Meter Performance

General performance of each of the meters was evaluated with respect to sensitivity, accuracy, stability, response, data acquisition requirements, cost, adequacy of manufacturer-supplied calibration information, and construction durability. With the exception of calibration and stability, these evaluations were based on manufacturer's data. A limited laboratory study was conducted initially to select a calibration specimen geometry and to investigate the effect of maximum aggregate size. A 0.15-m-diam by 0.54-m-long test specimen was selected to determine calibration factors for the meters. The results of these preliminary studies also indicated that the ratio of meter gage length to maximum aggregate size should be at least 3.5.

Calibration factors were determined for each of the 13 types of strain meters investigated. The tests were made on specimens each containing one embedment strain meter aligned with the cylinder axis. Just prior to testing, two 0.1-m wire-resistance strain meters were placed at 180° intervals on the specimen surface, and three sets of 0.2-m mechanical gage points were attached to the specimen surface at 120° intervals. The specimens were loaded in compression to failure. Embedded meter results were compared to the wire-resistance surface and the mechanical gage results as shown in Table 2. T2

The stability of the embedded strain meters was evaluated by using a copper-sealed cylindrical concrete test specimen, 0.41 m in diameter by 1.02 m long, as shown in Fig. 2. Contained within the cylinder were 18 embedment strain meters. Three weldable strain gages were attached at 120° intervals to a steel reinforcement gage which was used to maintain gage alignment during cylinder fabrication. Strain and temperature readings were monitored periodically while the cylinder was maintained F2

Table 1. Concrete embedment strain gages

Type	Gage length (cm)	Strain range (μm/m)	Temperature range (°C)	Sensitivity (μm/m)	Calibration factor	Readout requirements	Approximate cost/gage (U.S. $)	Comments
Electrical resistance								
Plastic encapsulated Type A	5–13	−20,000 to +15,000	−20 to +80	10	2.11	Strain indicator	5–20	Stability in moist environment questionable, volume change of plastic
Plastic encapsulated Type B	25	±20,000	−100 to +121	5–10	2	Strain indicator	50	Good resistance to grease and acids; stability in moist environment questionable
Single wire	5–15	±20,000	−200 to >315	5–10	2	Strain indicator	55–150	High-temperature use, small cross section requires careful placement
Unbonded wire Type A	10–25	3900	65	±5		Bridge circuit	35–75	Proven reliability
Unbonded wire Type B	10–25	+500 to −2000	−20 to +70	±6		Bridge circuit	35–40	Proven reliability
Unbonded wire Type C	5–10	±5000	−20 to +100	5–10	≈2.5	Strain indicator	50–70	Temperature compensated
Semiconductor[a]	0.16–0.3	+3000 to −10,000	−6 to +800		50–250	Bridge circuit	18–25	Very limited concrete applications, stable, high-temperature use, sensitive
Vibrating wire								
VWSG Type A	7–15	>1000	80	0.5	3.96×10^{-3}	Period or frequency meter	85–95	Used extensively, additional sealing recommended
VWSG Type B	17	>1000	80	0.5	3.00×10^{-3}	Period or frequency meter	75	Used extensively, additional sealing recommended
VWSG Type C	12.7	3000	−40 to +66	1.0	1	Period or frequency meter	150	Wire tension easily adjusted temperature measurement capability
VWSG Type D	13	3000		0.5	2.60×10^{-3}	Period or frequency meter	160	Temperature measurement capability, stability poor in moist environment
VWSG Type E	10	3000	−40 to +80	0.5	2.01×10^{-3}	Period or frequency meter	150	Temperature measurement capability
VWSG Type F	8.8	1000	−10 to +70	1	1.20×10^{-3}	Period or frequency meter	125	Temperature measurement capability
VWSG Type G	13.3	2000	−1	1	3.60×10^{-3}	Period or frequency meter	125–200	Temperature measurement capability
Inductance								
WES gage[a]	10.2	30,000				Carrier amplifier	200–300	Stable, low gage modulus limited number of gages fabricated

[a] Included for comparison purposes; gages of these types were not evaluated under this study.

[b] Strain determined from table supplied with gages which accounts for nonlinearities.

[c] May be specified for temperature range −30 to +200°C.

Table 2. Calibration results

Type	Range, % difference	Average, % difference
Vibrating wire strain gages		
VWSG Type A	−18.8 to −33.3	−25.7
VWSG Type B	−14.0 to −27.7	−20.9
VWSG Type C	−18.0 to −31.3	−26.4
VWSG Type D	+10.8 to +16.5	+13.7
VWSG Type E	−5.0 to −16.4	−10.7
VWSG Type F	−5.0 to −24.2	−13.1
VWSG Type G	−20.7 to −28.7	−25.7
Wire resistance strain gages		
Bonded wire		
Plastic encapsulated		
Type A	+1.4 to +10.0	+5.7
Type B	−8.0 to −11.3	−9.3
Single wire	−14.5 to −15.0	−14.8
Unbonded wire		
Type A	−11.8 to −19.2	−16.6
Type B	−9.8 to −20.4	−15.1
Type C	+7.0 to +13.5	+9.8

in a laboratory environment. Figures 3, 4, and 5 present results obtained for the bonded wire, unbonded wire and vibrating wire strain meters.

Meter Performance in Representative PCPV Environment

A second 0.41-m-diam by 1.02-m sealed concrete cylinder containing 12 embedment strain meters, three thermocouples, and three weldable strain gages, was used to evaluate meter performance in a simulated PCPV environment (Fig. 6). After curing for 3 months, the cylinder was heated using an insulated heating blanket. After an initial adjustment period, the temperature was maintained at 65 ± 5°C for approximately 6 months at which time axial compressive loading was applied to the cylinder. The specimen was loaded in increments of approximately 2.42 MPa with each loading increment maintained for 2 to 3 weeks. Temperature and strain readings

were monitored throughout the test. Figures 7 and 8 present results for the wire resistance and vibrating wire strain gages, respectively.

Meter Performance in Extreme Environments

Stability of the strain meters under severe environmental conditions was evaluated using water immersion tests. Samples of each of the 13 types of meters were subjected to sustained water immersion in baths at temperatures of 21 and 66°C as shown in Figs. 9 and 10, respectively. The test procedure consisted of placement of the meters in the appropriate alkaline (pH >9) water bath and periodically monitoring strain output. A summary of results obtained in this test series is presented in Table 3.

Conclusions

The results of the first phase of the evaluation of concrete embedment instrumentation indicate that: (1) meter selection should be based upon specific application, (2) calibration factors should be determined by embedding samples of the meters in test specimens fabricated using a representative concrete mix, (3) improved corrosion resistant materials and sealing techniques should be developed for meters which are to survive in PCPV environments, and (4) research should be conducted on other measurement techniques based on inductance, capacitance, and fluidic printiples. References 8 and 9 present more detailed results.

Grouted-Nongrouted Posttensioned Prestressing Systems

Under the structural models task, a study was conducted to investigate the relative merits of grouted and nongrouted posttensioned prestressing systems for PCPVs. A literature review was included in the investigation to: provide insight into the behavior of grouted tendon systems, establish performance histories for structures using grouted and nongrouted tendon systems, identify corrosion protection procedures for prestressing tendons, identify arguments both for and against grouting tendons, and to aid in the development of the experimental investigation. The experimental investigation for which results will be

Table 3. Results of alkaline-water immersion test

Gage type	Room-temperature water bath			Elevated-temperature water bath		
	Number tested	Number and type of failure[a]		Number tested	Number and type of failure[a]	
		a	b		a	b
Unbonded wire						
Type A	4	0	0	8	2	1
Type B	2	0	0	2	0	0
Type C	1	0	0	1	0	0
Polyester encapsulated						
Type A	3	3	0	6	6	0
Type B	6	6	0	0	0	0
Single wire	9	4	0	16	7	0
Vibrating wire						
Type A[b]	3	0	1	3	0	1
Type B[b]	1	0	1	0	0	0
Type C	2	0	0	2	0	[c]
Type D	2	0	2	1	0	1
Type E	1	1	0	1	0	1
Type F	3	0	0	4	0	1
Type G	2	0	0	3	0	2

[a]Type of failure: a = excessive strain; b = no reading obtainable. Excessive strain failure by definition is a strain in excess of a 3-με/day drift rate. This value was arbitrarily selected and may be too lax in some cases and too stringent in others.

[b]Tested as received; manufacturer recommends additional sealing.

[c]Erratic readings at temperatures greater than manufacturer's stated upper limit.

presented was divided into three phases: (1) grouted-nongrouted tendon behavior, (2) evaluation of selected "new" materials, and (3) corrosion study.

Grouted-Nongrouted Tendon Behavior

The basic test member for this study was a 0.15-m-wide by 0.30-m-deep by 3.1-m-long beam containing one 7-wire prestressing strand conforming to ASTM A416-74 grade 270. The percent of prestressing (0.5, 0.6, and 0.7) strand ultimate strength and loading rate (74 N/s to 74 kN/s) were selected as the test variables. The influence of level of prestressing and rate of loading on the load-centerline deflection of the grouted and nongrouted tendon beams tested to failure in flexure are shown in Figs. 11 and 12, respectively. The results also indicated that: beams having grouted tendons developed more cracks, but the cracks are of smaller width; as the level of prestressing increased, the ultimate load capacity and the load at which first cracking occurred increased; and the ultimate load capacity of beams having grouted tendons was higher than that for beams having nongrouted tendons at the same level of prestressing.

New Materials Evaluation

Fibrous concrete and polymer-silica cement, two materials somewhat new to PCPV applications, were evaluated. Beam structural members having the same geometry as those in the previous section were fabricated using a fibrous concrete mix which contained 1.5% 1-in. steel fibers by volume. Both grouted and nongrouted fibrous concrete beams were tested to failure in flexure, and results obtained indicate that the addition of the fibers increases the ductility of the beams. Fibrous concrete potentially has application in areas of stress concentration such as at penetrations to reduce steel congestion.

Polymer-silica cements, which are inorganic corrosion resistant materials, were investigated for elevated temperature applications where their desirable properties of rapid strength development, nonshrinking, good bond to minerals, and high temperature could be utilized. Limited

results obtained from 25.4-mm cube specimens which were subjected to temperatures up to 816°C for exposure periods from 3 days to 56 days show that when the material system is subjected to elevated-temperature exposures up to 538°C, there are significant increases in compressive strength and moduli of elasticity values relative to values obtained for specimens maintained at room temperature. Increases in these values were also obtained for exposures to 816°C for periods less than 7 days.

Corrosion Study

The purpose of this study was to determine the corrosion behavior of a high-strength steel (ASTM A416-74 grade 270), typical of those used as tendon materials in prestressed concrete pressure vessels, in several corrosive environments and to demonstrate the protection afforded by coating the steel with either of two commercial organic petrolatum-based greases or portland cement grout. The study utilized 305-mm-long segments from the center, straight wire of a 7-wire prestressing strand which was either stressed or unstressed while subjected to the corrosive environment. Variables in the investigation were stress level [0–90% of wire ultimate tensile strength (UTS)], coating materials (none, cement grout, selected commercial products), time of exposure (0.29–3790 h), and environment [hydrogen-sulfide saturated water at room temperature (3000 ppm, ph ∿4), 0.2 *M* NH_4NO_3 at 66°C, and 0.1 *M* NaCl at room temperature].

The test setup for the stressed tendon test series is shown in Fig. 13. Hydrogen-sulfide saturated water was the only corrosive medium investigated in this series. (The severity of this environment is shown in Fig. 14 which presents the effect of level of stress on time to failure for unprotected wire.) Specimens in this series were protected by either petrolatum- or portland cement-based coatings while loaded to 60% UTS. The effect of flaws in the coating materials was also investigated. None of the specimens protected by unflawed coatings cracked during approximately 6 days of exposure, and subsequent tensile tests showed that no degradation of either load capacity or ductility had occurred. The organic materials demonstrated the ability to heal coating discontinuities, and flaw widths up to 0.1-mm wide can be contained in the grout without detrimental effects.

Fl

Fl

Protected and unprotected wires in the unstressed test series were exposed to solutions of 0.1 *M* hydrogen sulfide and 0.1 *M* NaCl at room temperature and 0.2 *M* NH_4NO_3 at 66°C. The test fixture for containing the specimens exposed to the hydrogen sulfide environment is shown in Fig. 15 and that for the specimens subjected to the NaCl and NH_4NO_3 solutions in Fig. 16. Periodically specimens were removed from their test fixtures and tested in tension to failure at a cross-head velocity of 0.51 mm/min. Unprotected wires subjected to these environments exhibited significant reductions in both UTS and ductility. Coated wires exposed to the H_2S saturated water for up to 120 days showed little or no reductions in UTS and ductility, but the presence of flaws in the coatings produced significant reductions. Specimens protected by organic coatings with and without flaws exhibited no reduction in either UTS or ductility after 132 days of exposure to the NH_4NO_3 solution; however, grout protected specimens showed increasing reductions in UTS and ductility with increased lengths of exposure (presence of flaws in the grout accelerated these reductions). Decreases in UTS and ductility of 5—7% occurred in specimens protected by coatings with and without flaws (grout flaw widths <3.18 mm) after 164 days of exposure to the NaCl solution.

General conclusions derived from this study are that: (1) prestressing materials should be continuously protected from time of manufacture, (2) exclusion of sulfide, nitrate, and chloride environments is required to prevent reduction in mechanical properties of prestressing, and (3) both portland cement and organic petrolatum-based corrosion inhibitors when properly applied provide positive exclusion of corrosive environments from prestressing materials.

Structural Integrity Monitoring by Acoustic Emission

Acoustic emissions are small amplitude elastic stress waves generated during material deformation resulting from thermal or mechanical stimulus. The stress waves are detected by transducers as small displacements on the specimen surface. Characterization of these stress wave emissions provides insight into the type of inelastic deformation occurring -- amplitude indicates the magnitude of flaw extension; rate of emission indicates flaw propagation velocity; and the total acoustic emission energy

generated is proportional to the loss of structural integrity. Present generation computer controlled acoustic emission systems such as shown in Fig. 17 are not only able to detect these emissions but also to locate their source. Results obtained from basic acoustic emission studies conducted in the laboratory and the field are sufficiently encouraging to indicate that this technique has potential for structural integrity monitoring of PCPVs. Studies have been initiated under our PCPV program to demonstrate the capability of acoustic emission. To date these studies have been confined to monitoring of prestressed concrete beams described previously.

Selected beams of the grouted-nongrouted tendon test series were monitored by acoustic emission while tested to failure. The test procedure consisted of: attaching four 50-kHz acoustic emission transducers to the bottom of the beam, calibration of the acoustic emission equipment, and loading the beam to failure in flexure. Figures 18 and 19 present typical acoustic emission results for a grouted and nongrouted tendon beam. Superimposed above the acoustic emission activity plots are photographed of the beams after testing so that agreement between crack locations and acoustic emission active areas may be noted. Results indicate that acoustic emission is able to locate cracks in prestressed concrete structures; however, as the cracks increase in number and branch, the acoustic emission active regions "smear."

RECENT EXPERIMENTAL STUDIES OF PCRV CLOSURES

Analytical and experimental studies of the ~~closures~~ PCPV core cavity closures shown in Fig. 20 for both the steam generator and central ~~reactor cavities~~ are being conducted. The program involves (1) relatively small 1:15-scale closure plug models, (2) more detailed 1:4-scale closure plugs in which the plug, seal, and hold-down system are modeled, and (3) a 1:10-scale model of the entire PCPV. Thus far, full- and half-thickness 1:15-scale models of the steam-generator cavity closure plugs have been tested.

Full-Thickness Plug Model

The prototype steam-generator cavity closure plug is shown in Fig. 21. A cross section of the model positioned ready for testing in the steel test fixture (cross hatching) is shown in Fig. 22. The primary difference between the model and prototype is in the restraint provided by their associated hold-down systems. A ball-bearing support system was selected to provide sufficient support for the model to preclude premature failure during the overpressurization phase of the test. Although less radial compression is probably produced on the model forging by the ball-bearing support system, analysis results indicate that the difference is quite small.

The model was subjected to 10 pressurization cycles to 10.08 MPa (maximum cavity pressure) with the pressure reduced to 2.07 MPa between cycles. The final loading cycle was to be to failure; however, the test was stopped at 75.8 MPa (7.5 times design pressure of prototype) to avoid damaging the hold-down system. At this pressure the concrete and steel components both exhibited significant nonlinearities in strain and deformation. Figure 23 presents a cross section of the plug model after testing. Reference 10 presents more details of the test.

Half-Thickness Plug Model

Since both the calculated and experimental results indicated that the plug was overdesigned, a second model having reduced thickness was tested. Basic changes in the second model were as follows: (1) thickness reduced to one half that of the first model, (2) steel plate-type shear reinforcement was eliminated, and (3) rebar layout was changed to eliminate the middle section which had been designed to allow for the presence of the shear reinforcement. Figure 24 presents the one-half thickness model prior to casting of the microconcrete.

The test plan for the second model was identical to the first model. After being subjected to 10 pressurization cycles of from 2.8 MPa to the maximum cavity pressure, the model was pressurized in steps to failure, which occurred at approximately 99 MPa. As shown in Fig. 25, the failure occurred by punching shear along a roughly conical failure surface.

Conclusions

The two closure tests conducted to date have indicated that: (1) the plugs have high ultimate loads with large pressure capacities, (2) present designs are adequate but conservative, (3) failures are of the punching shear type, and (4) satisfactory analyses will require the development of improved constitutive equations for concrete.

PCPV PROGRAM SUMMARY

A comprehensive program in support of PCRV development is under way at the Oak Ridge National Laboratory. Both analytical and experimental studies are included. Under the analytical studies, improved concrete constitutive equations have been developed for modern 3-dimensional finite-element codes. An extensive experimental study of the ultimate capacity of PCRV head regions has been completed. Studies of embedment strain instrumentation and grouted prestressing tendons have also been completed. Acoustic emission has been shown to be a promising technique for structural monitoring of PCPVs. Projects planned for the future include the development of an optimized PCRV and a model test of the proposed offset core PCRV design. We have initiated projects to develop improved cracking analysis techniques and capability for testing heated concrete under various combinations of multiaxial stress.

Under the GCFR-sponsored program, we have tested two models of proposed steam-generator cavity closure designs. We are currently planning to conduct similar tests for the core cavity closure.

REFERENCES

1. Z. P. Bazant, et al., *Endochronic Theory for Inelasticity and Failure Analysis of Concrete Structures*, Structural Engineering Report No. 1976-12/259, Northwestern University (December 1976).

2. R. K. Nanstad, *A Review of Concrete Properties for Prestressed Concrete Pressure Vessels*, ORNL/TM-5497 (October 1976).

3. T. W. Kennedy, *Long-Term Creep Behavior of Concrete*, Research Report 3899-1, University of Texas (January 1975).

4. J. E. McDonald, *Time-Dependent Deformation of Concrete Under Multiaxial Stress Conditions*, Technical Report C-75-4, U.S. Army Engineer Waterways Experiment Station (October 1975).

5. J. P. Callahan, et al., *Prestressed Concrete Reactor Vessel Thermal Cylinder Model Study*, ORNL/TM-5613 (June 1977).

6. J. E. McDonald, *Moisture Migration in Concrete*, Technical Report C-75-1, U.S. Army Engineer Waterways Experiment Station (May 1975).

7. D. A. Canonico, *Second Interim Report on PCRV Thermal Cylinder Axial Tendon Failures*, ORNL-TM-4764 (November 1974).

8. D. J. Naus and C. C. Hurtt, *Monitoring of Prestressed Concrete Pressure Vessels. 1. An Overview of Concrete Embedment Strain Instrumentation and Calibration Test Results for Selected Concrete Embedment Strain Meters*, ORNL/TM-6191/V1 (June 1978).

9. D. J. Naus and C. C. Hurtt, *Monitoring of Prestressed Concrete Pressure Vessels. 2. Performance of Selected Concrete Embedment Strain Meters Under Normal and Extreme Environmental Conditions*, ORNL/TM-6191/V2 (October 1978).

10. W. G. Dodge, et al., *GCFR 1/15-Scale PCRV Steam-Generator Cavity Closure Model Test*, ORNL/TM-6005 (April 1978).

FIGURE CAPTIONS

Fig. 1. Basic program activities.

Fig. 2. Meter stability test specimen.

Fig. 3. Bonded wire resistance meter stability test results.

Fig. 4. Unbonded wire resistance meter stability test results.

Fig. 5. Vibrating wire meter stability test results.

Fig. 6. Simulated PCPV environment test setup.

Fig. 7. Wire resistance meters simulated PCPV test results.

Fig. 8. Vibrating wire meters simulated PCPV test results.

Fig. 9. Room temperature alkaline-water bath.

Fig. 10. Elevated temperature alkaline-water bath.

Fig. 11. Effect of prestressing level on load-centerline deflection.

Fig. 12. Effect of loading rate on load-centerline deflection. (a) Grouted tendon beams, (b) nongrouted tendon beams.

Fig. 13. Stressed tendon corrosion test setup.

Fig. 14. Effect of level of stress on time to failure for unprotected wire.

Fig. 15. Unstressed tendon corrosion test setup — H_2S environment.

Fig. 16. Unstressed tendon corrosion test setup — NH_4NO_3 and NaCl environments.

Fig. 17. Multichannel acoustic emission source location system.

Fig. 18. Acoustic emission results — grouted tendon beam.

Fig. 19. Acoustic emission results — nongrouted tendon beam.

Fig. 20. Closures investigated under the GCFR Program.

Fig. 21. Prototype steam-generator cavity closure plug.

Fig. 22. Model position in test fixture.

Fig. 23. Full-thickness model cross section after testing.

Fig. 24. Half-thickness model prior to casting microconcrete.

Fig. 25. Half-thickness model after testing.

THE FOUR BASIC PROGRAM ACTIVITIES ARE CLOSELY TIED TO ONGOING PCRV DESIGN DEVELOPMENT.

ORNL DWG 78-8437

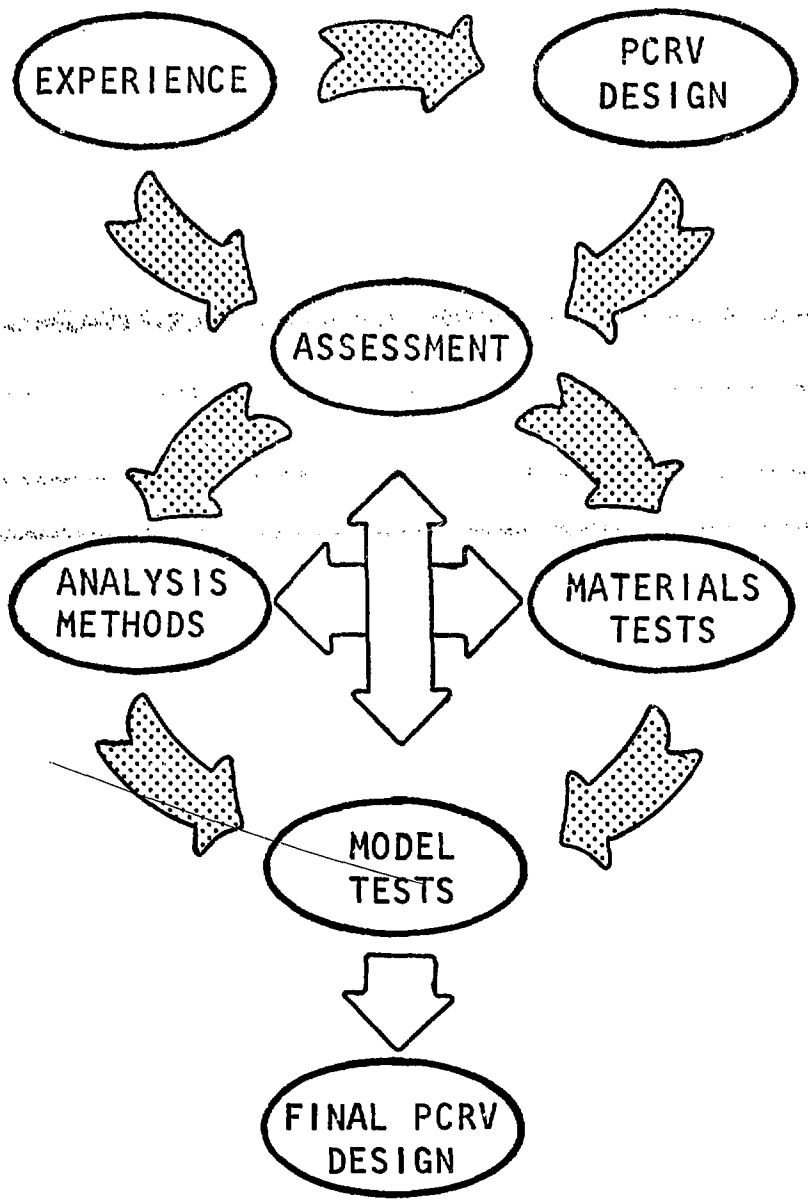

GAGE STABILITY TEST SPECIMEN

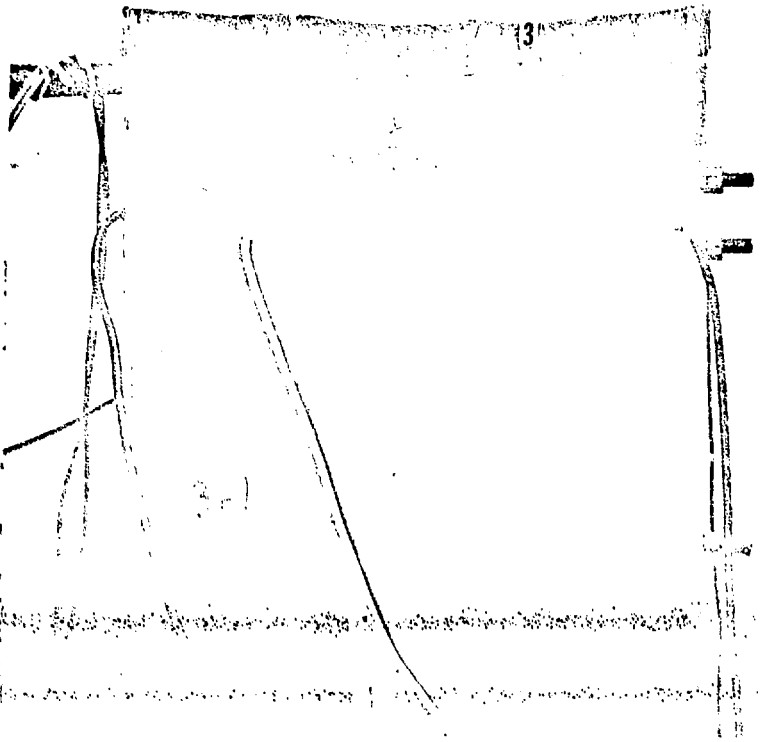

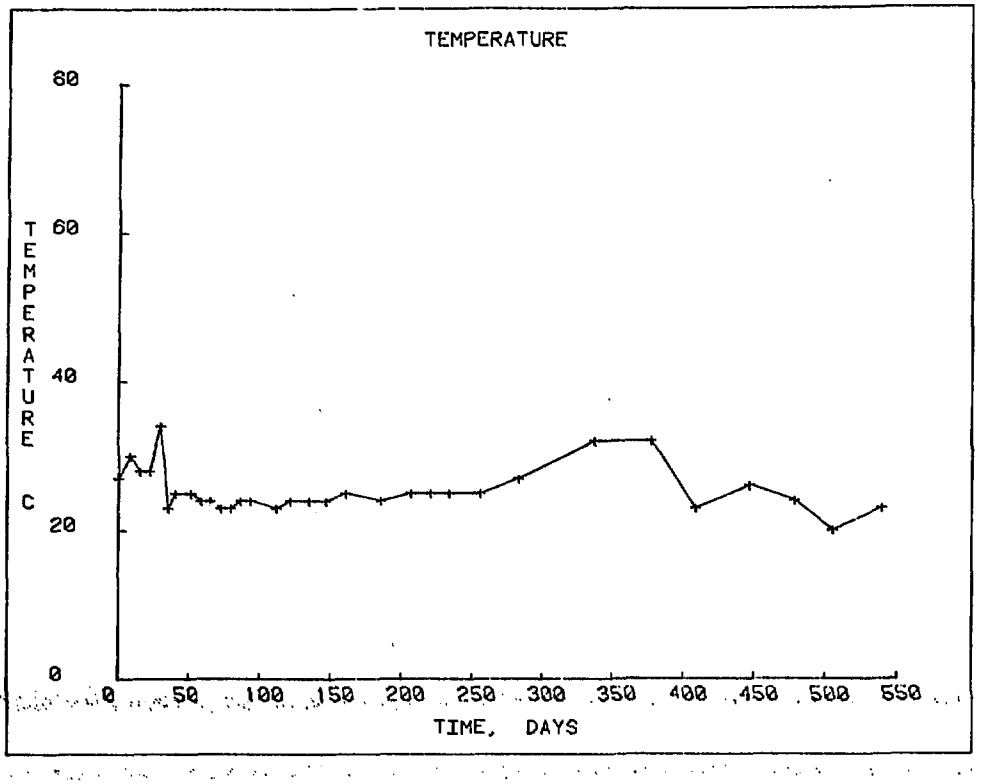
TEMPERATURE
TEMPERATURE C
60
60
40
20
0
0
50
100
150
200
250
300
350
400
450
500
550
TIME, DAYS

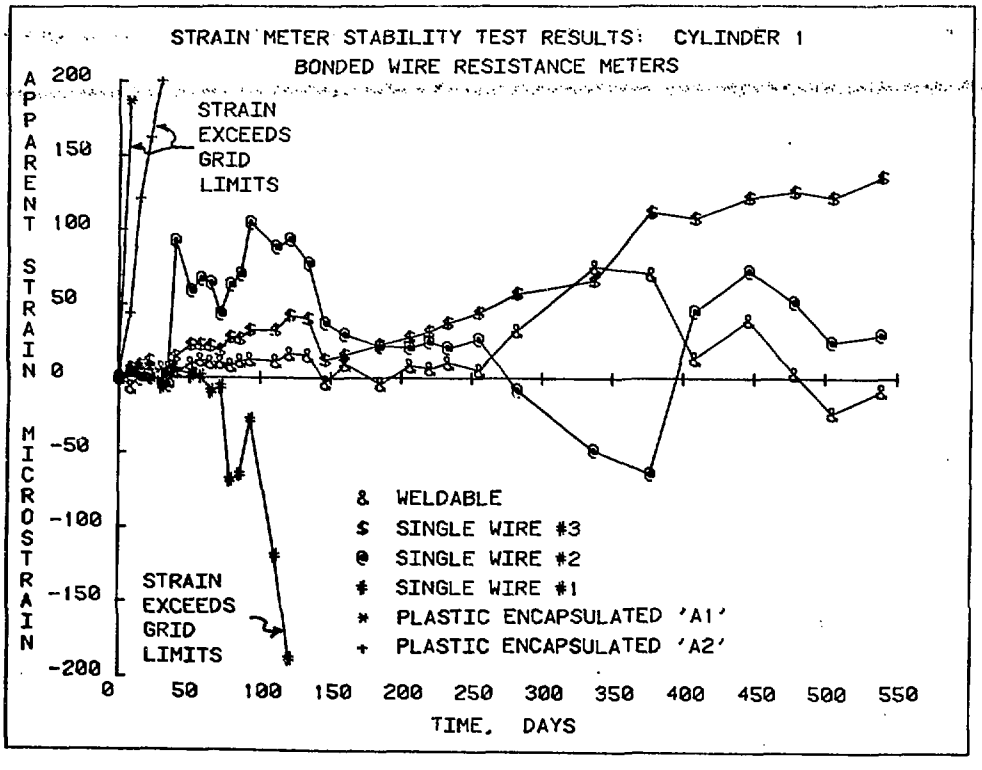
STRAIN METER STABILITY TEST RESULTS: CYLINDER 1
BONDED WIRE RESISTANCE METERS
APPARENT STRAIN MICROSTRAIN
200
150
100
50
0
-50
-100
-150
-200
STRAIN EXCEEDS GRID LIMITS
STRAIN EXCEEDS GRID LIMITS
& WELDABLE
$ SINGLE WIRE #3
@ SINGLE WIRE #2
# SINGLE WIRE #1
* PLASTIC ENCAPSULATED 'A1'
+ PLASTIC ENCAPSULATED 'A2'
0
50
100
150
200
250
300
350
400
450
500
550
TIME, DAYS

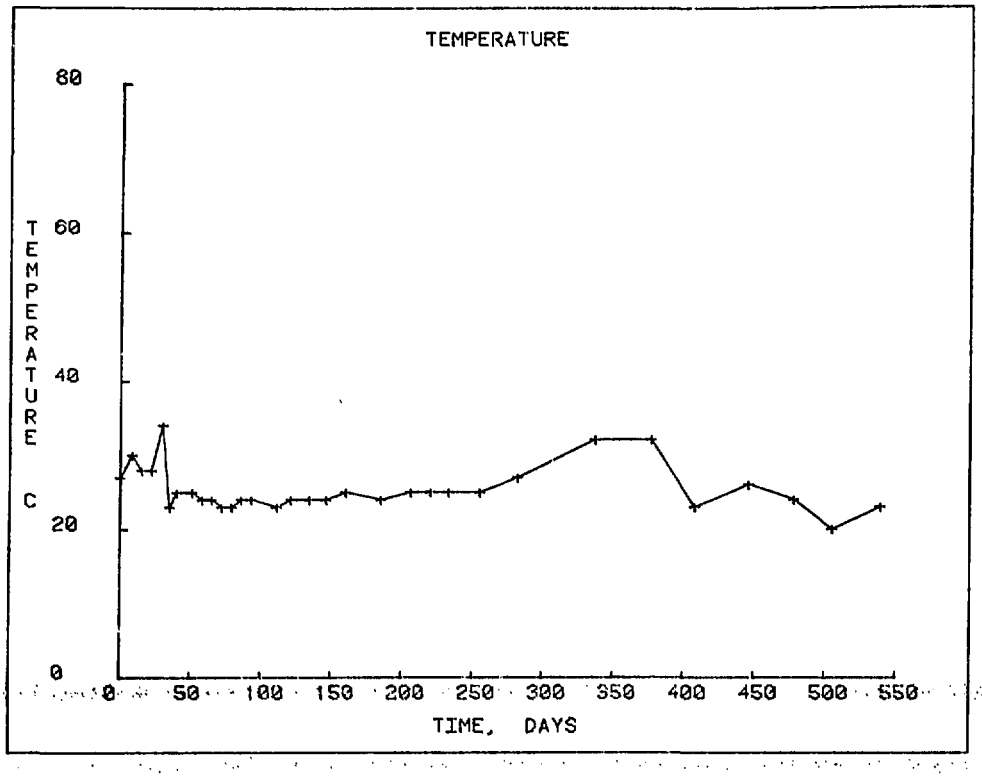
TEMPERATURE
TEMPERATURE C
80
60
40
20
0
0
50
100
150
200
250
300
350
400
450
500
550
TIME, DAYS

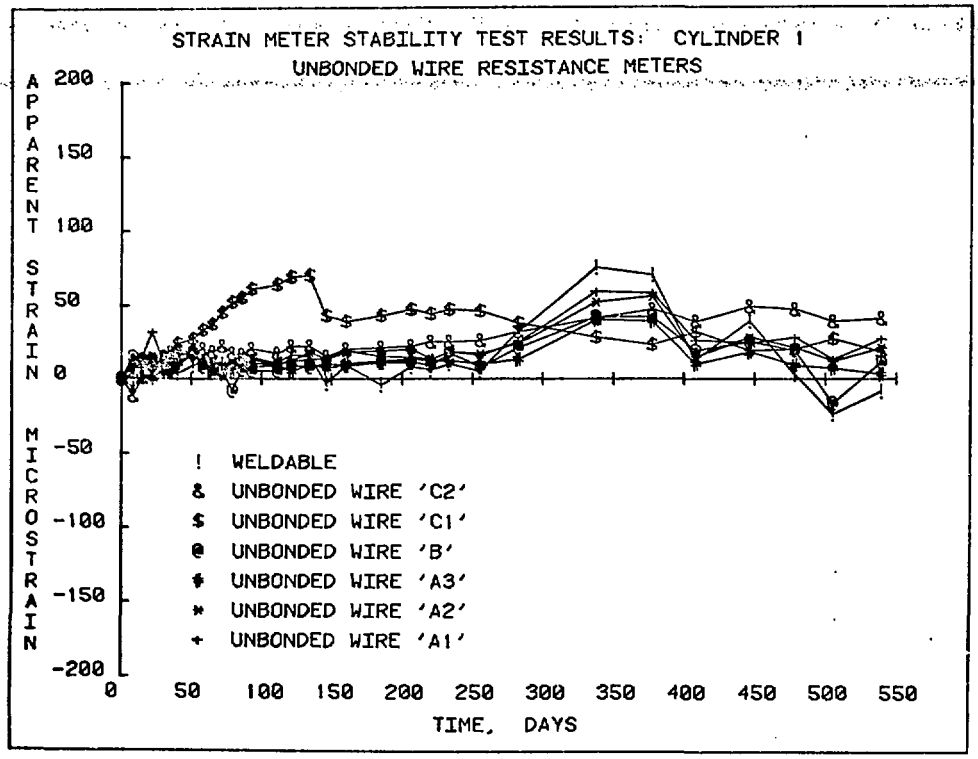
STRAIN METER STABILITY TEST RESULTS: CYLINDER 1
UNBONDED WIRE RESISTANCE METERS
APPARENT STRAIN MICROSTRAIN
200
150
100
50
0
-50
-100
-150
-200
! WELDABLE
& UNBONDED WIRE 'C2'
$ UNBONDED WIRE 'C1'
@ UNBONDED WIRE 'B'
# UNBONDED WIRE 'A3'
* UNBONDED WIRE 'A2'
+ UNBONDED WIRE 'A1'
0
50
100
150
200
250
300
350
400
450
500
550
TIME, DAYS

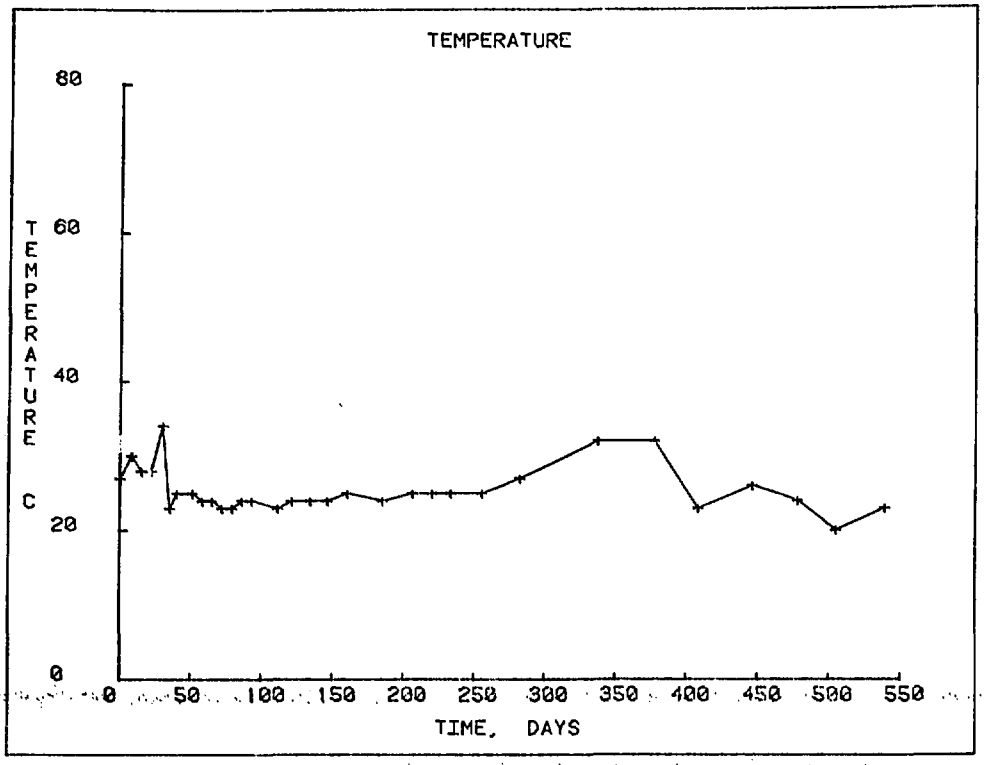
TEMPERATURE
TEMPERATURE C
80
60
40
20
0
0
50
100
150
200
250
300
350
400
450
500
550
TIME, DAYS

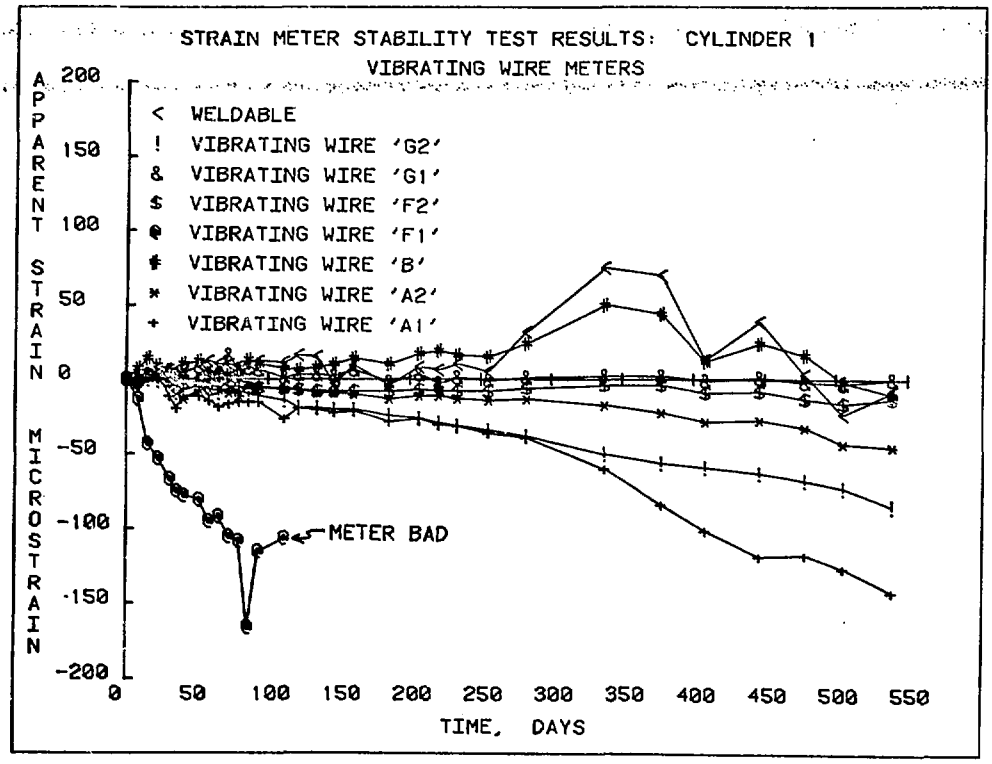
STRAIN METER STABILITY TEST RESULTS: CYLINDER 1
VIBRATING WIRE METERS
APPARENT STRAIN MICROSTRAIN
200
150
100
50
0
-50
-100
-150
-200
< WELDABLE
! VIBRATING WIRE 'G2'
& VIBRATING WIRE 'G1'
$ VIBRATING WIRE 'F2'
@ VIBRATING WIRE 'F1'
# VIBRATING WIRE 'B'
* VIBRATING WIRE 'A2'
+ VIBRATING WIRE 'A1'
METER BAD
0
50
100
150
200
250
300
350
400
450
500
550
TIME, DAYS

REPRESENTATIVE PCPV ENVIRONMENT TEST SETUP

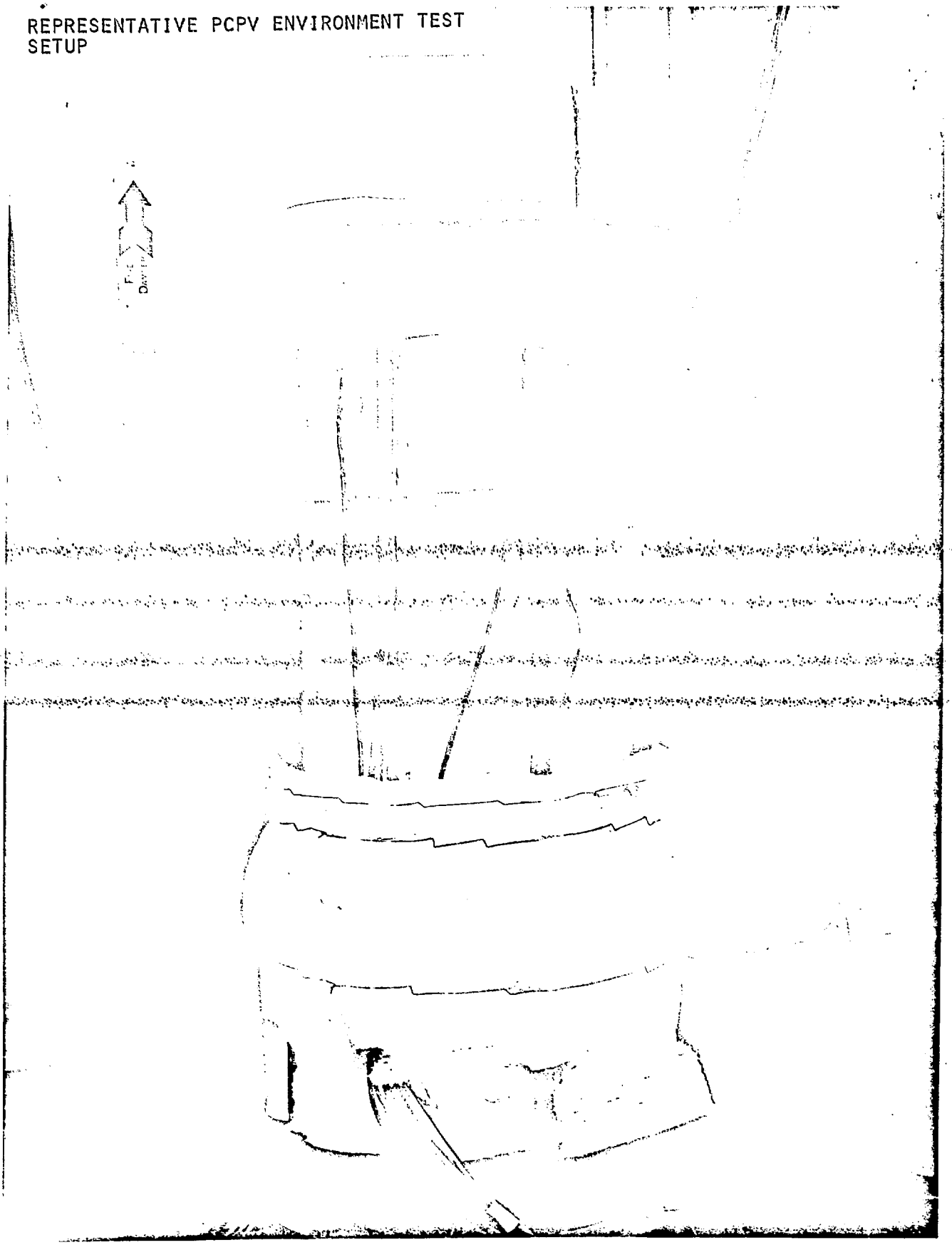

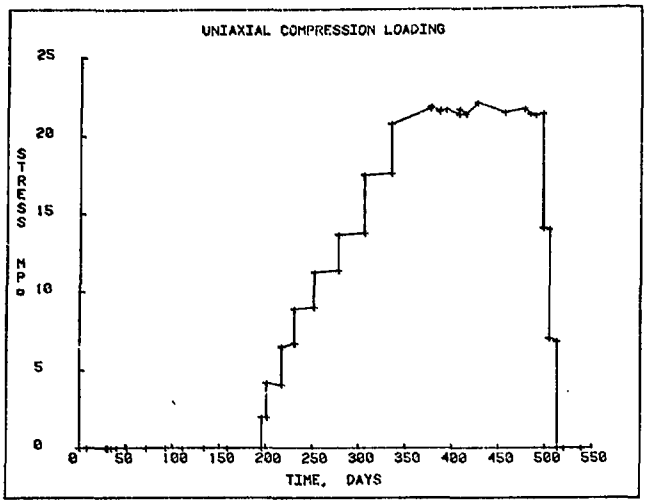
UNIAXIAL COMPRESSION LOADING
STRESS MPa
25
20
15
10
5
0
0 50 100 150 200 250 300 350 400 450 500 550
TIME, DAYS

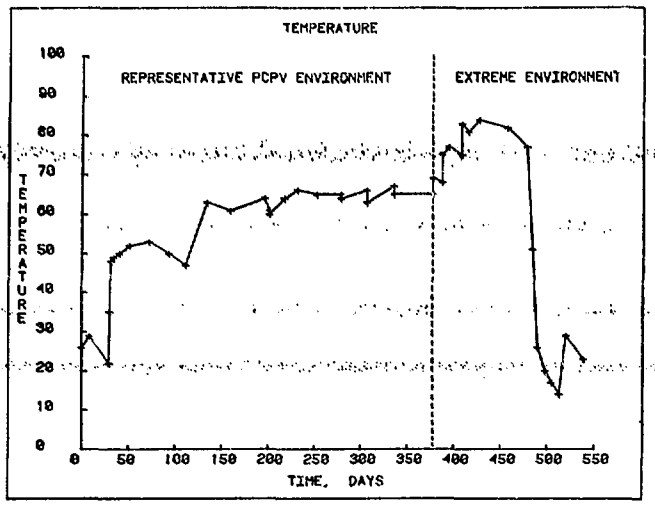
TEMPERATURE
REPRESENTATIVE PCPV ENVIRONMENT
EXTREME ENVIRONMENT
TEMPERATURE
100
90
80
70
60
50
40
30
20
10
0
0 50 100 150 200 250 300 350 400 450 500 550
TIME, DAYS

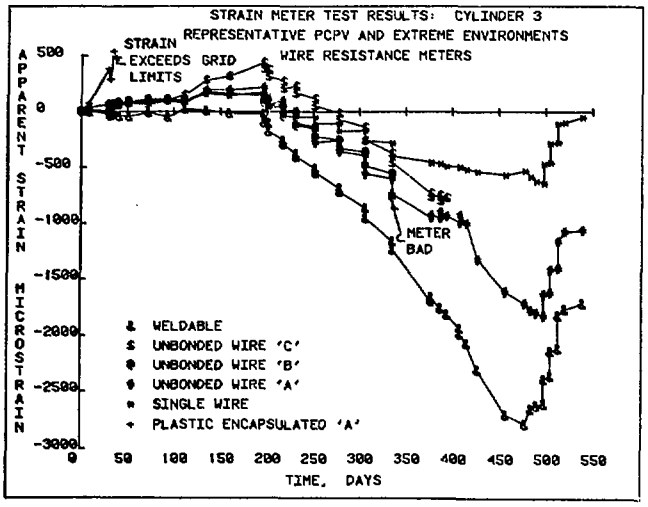
STRAIN METER TEST RESULTS: CYLINDER 3
REPRESENTATIVE PCPV AND EXTREME ENVIRONMENTS
WIRE RESISTANCE METERS
STRAIN EXCEEDS GRID LIMITS
METER BAD
APPARENT STRAIN MICROSTRAIN
500
0
-500
-1000
-1500
-2000
-2500
-3000
& WELDABLE
$ UNBONDED WIRE 'C'
@ UNBONDED WIRE 'B'
¢ UNBONDED WIRE 'A'
* SINGLE WIRE
+ PLASTIC ENCAPSULATED 'A'
0 50 100 150 200 250 300 350 400 450 500 550
TIME, DAYS

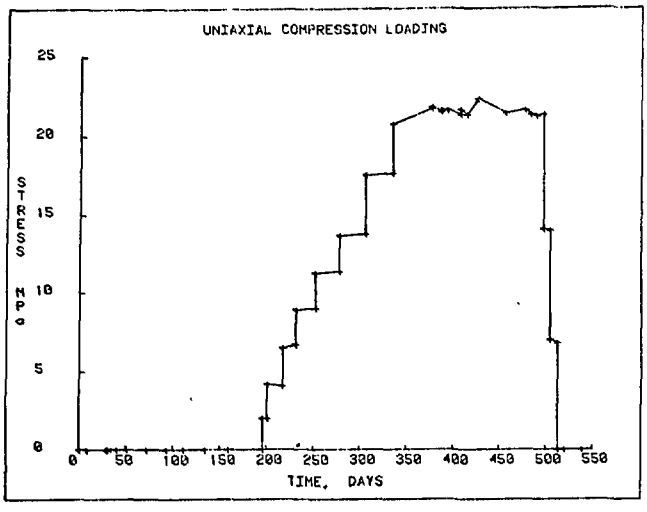
UNIAXIAL COMPRESSION LOADING
STRESS MPa
0
5
10
15
20
25
0
50
100
150
200
250
300
350
400
450
500
550
TIME, DAYS

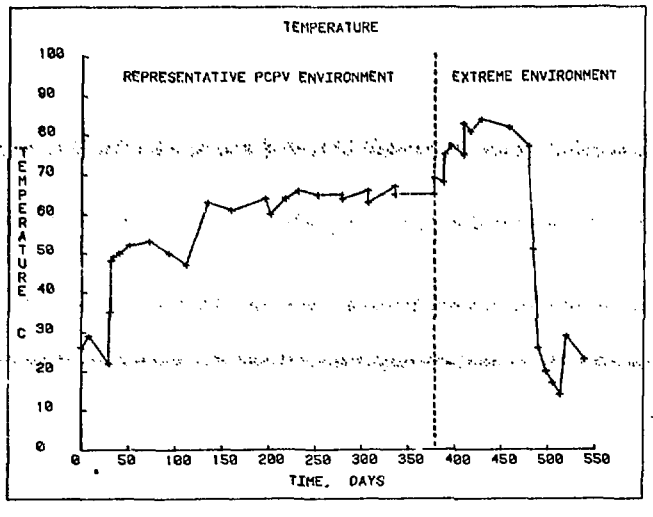
TEMPERATURE
REPRESENTATIVE PCPV ENVIRONMENT
EXTREME ENVIRONMENT
TEMPERATURE C
0
10
20
30
40
50
60
70
80
90
100
0
50
100
150
200
250
300
350
400
450
500
550
TIME, DAYS

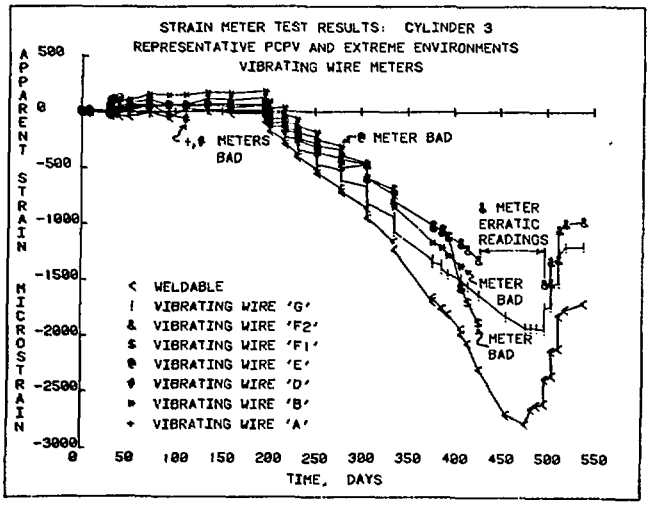
STRAIN METER TEST RESULTS: CYLINDER 3
REPRESENTATIVE PCPV AND EXTREME ENVIRONMENTS
VIBRATING WIRE METERS
APPARENT STRAIN MICROSTRAIN
500
0
-500
-1000
-1500
-2000
-2500
-3000
+,$ METERS BAD
@ METER BAD
& METER ERRATIC READINGS
METER BAD
METER BAD
< WELDABLE
! VIBRATING WIRE 'G'
& VIBRATING WIRE 'F2'
$ VIBRATING WIRE 'F1'
@ VIBRATING WIRE 'E'
# VIBRATING WIRE 'D'
= VIBRATING WIRE 'B'
+ VIBRATING WIRE 'A'
0
50
100
150
200
250
300
350
400
450
500
550
TIME, DAYS

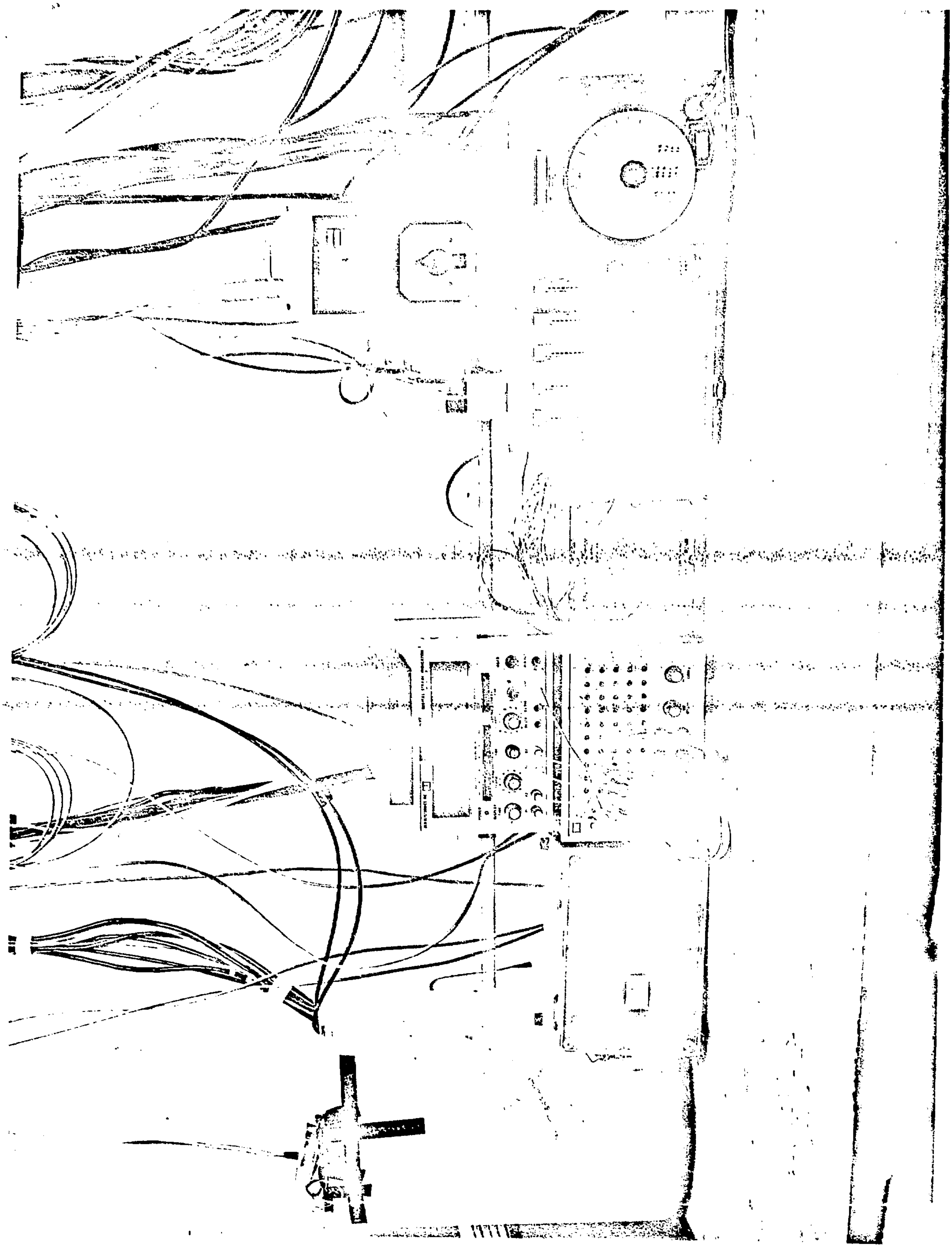

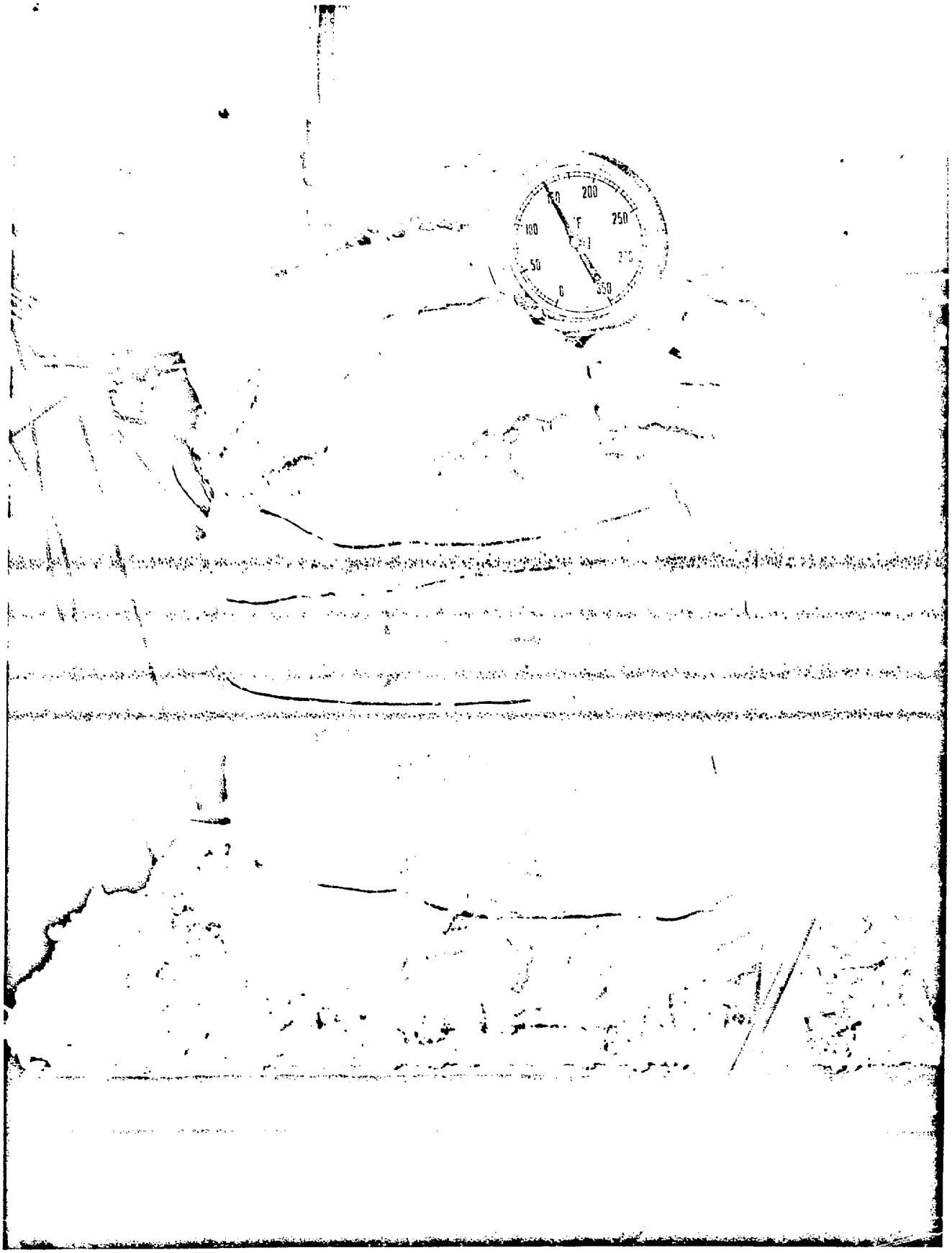
150
200
250
100
°F
50
0
350

ULTIMATE LOAD CAPACITY OF PRESTRESSED CONCRETE BEAMS IS IMPROVED SIGNIFICANTLY BY GROUTING THE TENDONS.

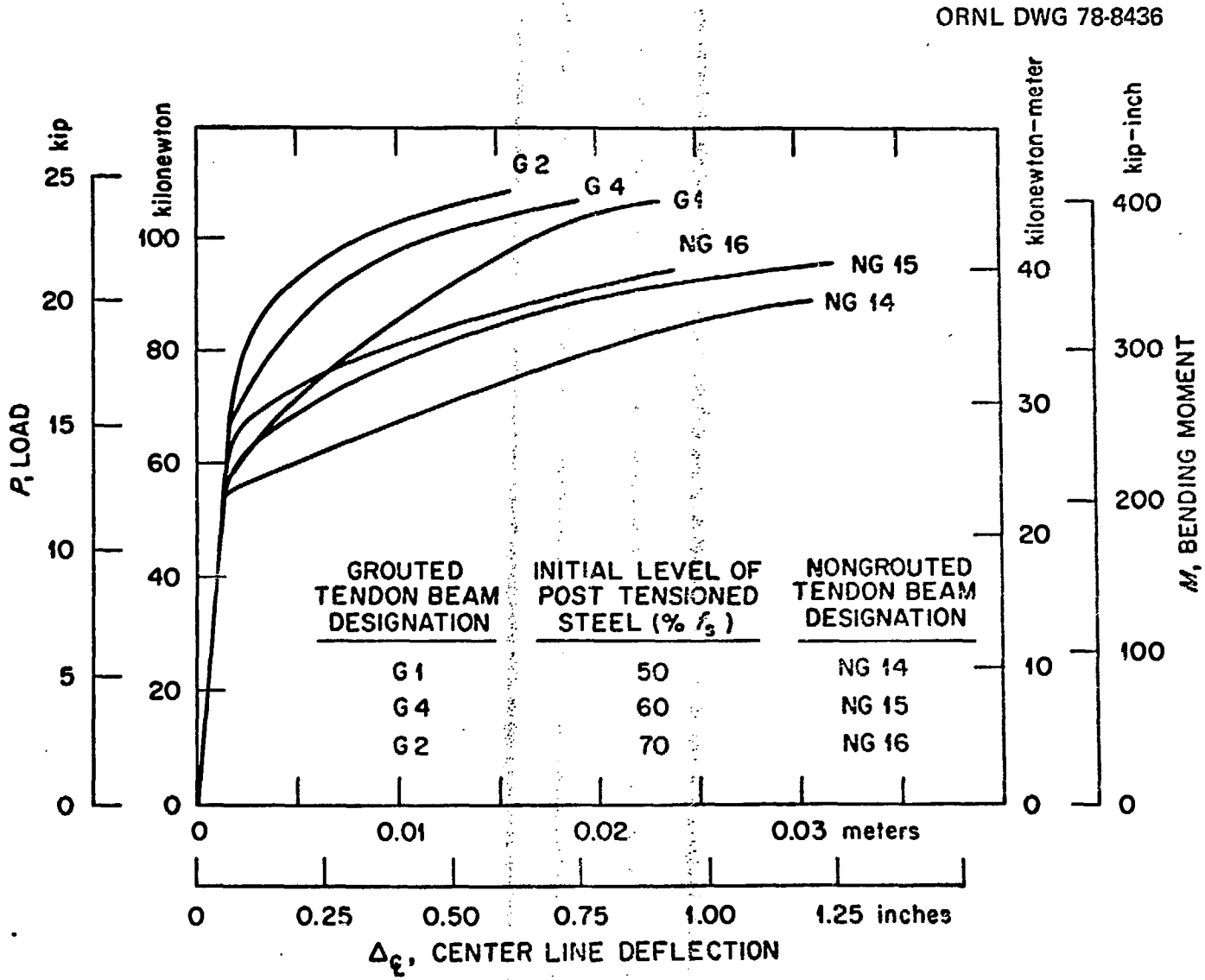

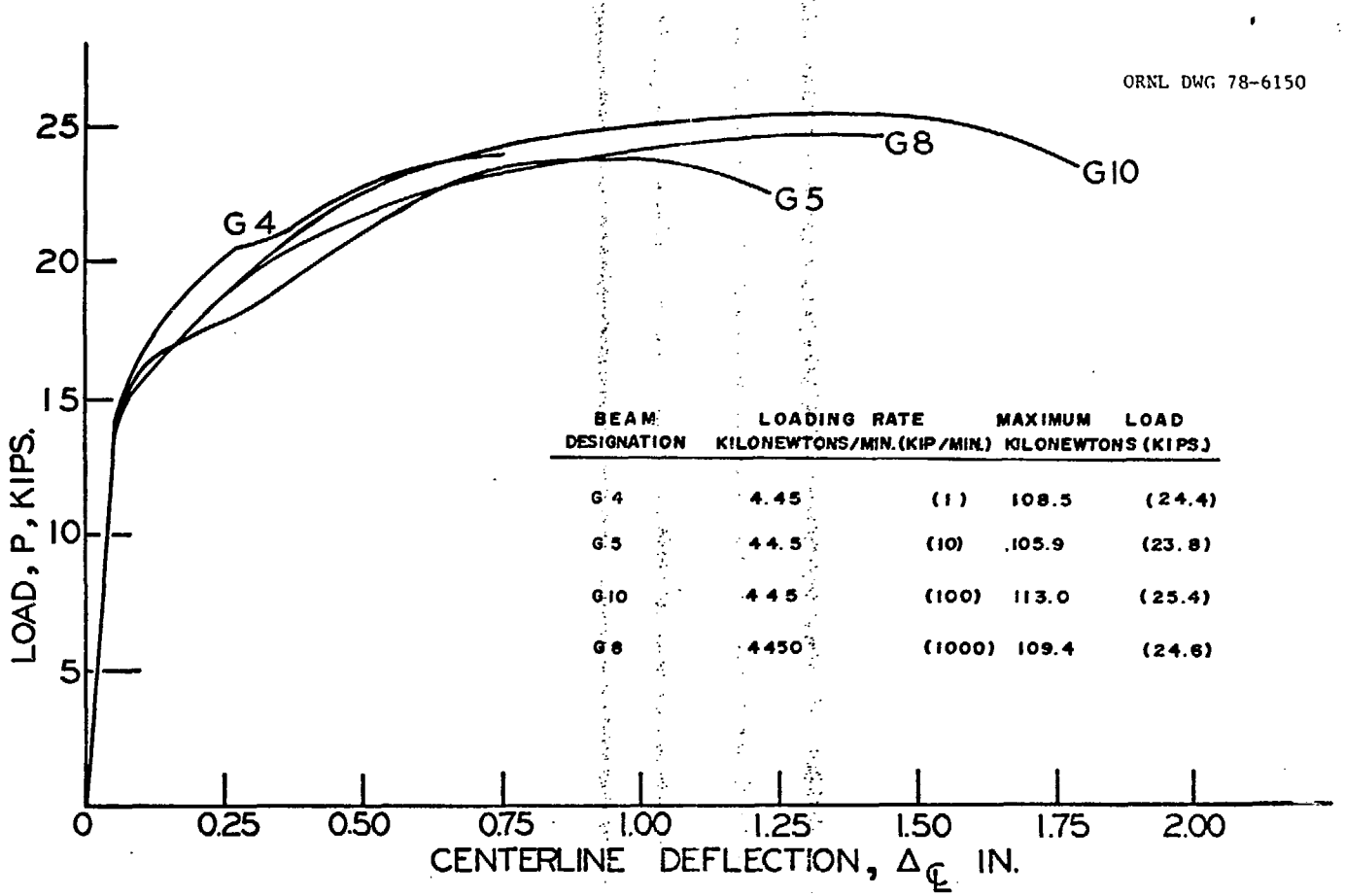

BEAM DESIGNATION	LOADING RATE KILONEWTONS/MIN.	(KIP/MIN.)	MAXIMUM LOAD KILONEWTONS	(KIPS)
G-4	4.45	(1)	108.5	(24.4)
G-5	44.5	(10)	105.9	(23.8)
G-10	445	(100)	113.0	(25.4)
G-8	4450	(1000)	109.4	(24.6)

EFFECT OF LOADING RATE: GROUTED TENDON BEAMS

ORNL DWG 78-6149

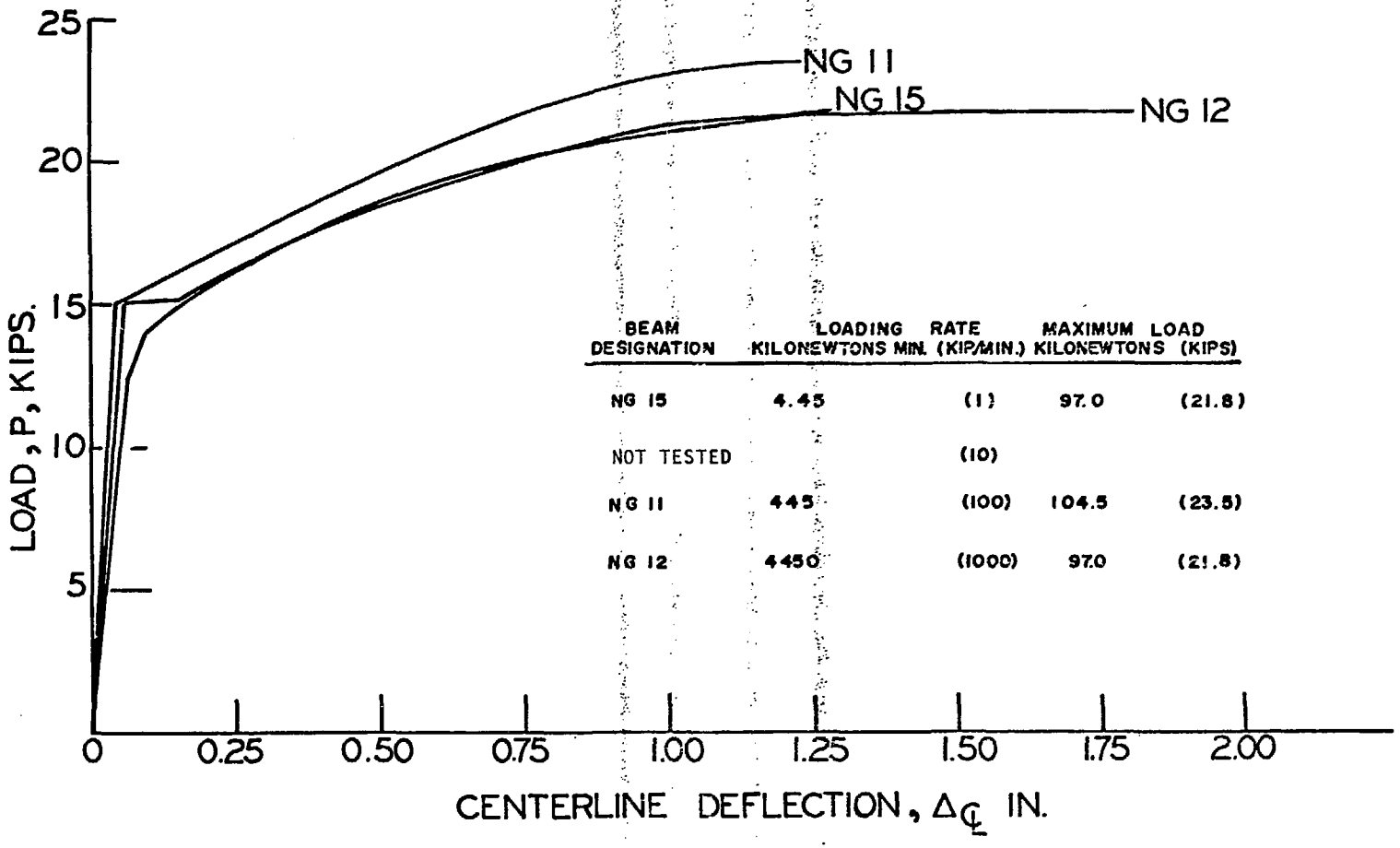

BEAM DESIGNATION	LOADING RATE KILONEWTONS MIN.	(KIP/MIN.)	MAXIMUM LOAD KILONEWTONS	(KIPS)
NG 15	4.45	(1)	97.0	(21.8)
NOT TESTED		(10)		
NG 11	445	(100)	104.5	(23.5)
NG 12	4450	(1000)	97.0	(21.8)

EFFECT OF LOADING RATE: NONGROUTED TENDON BEAMS

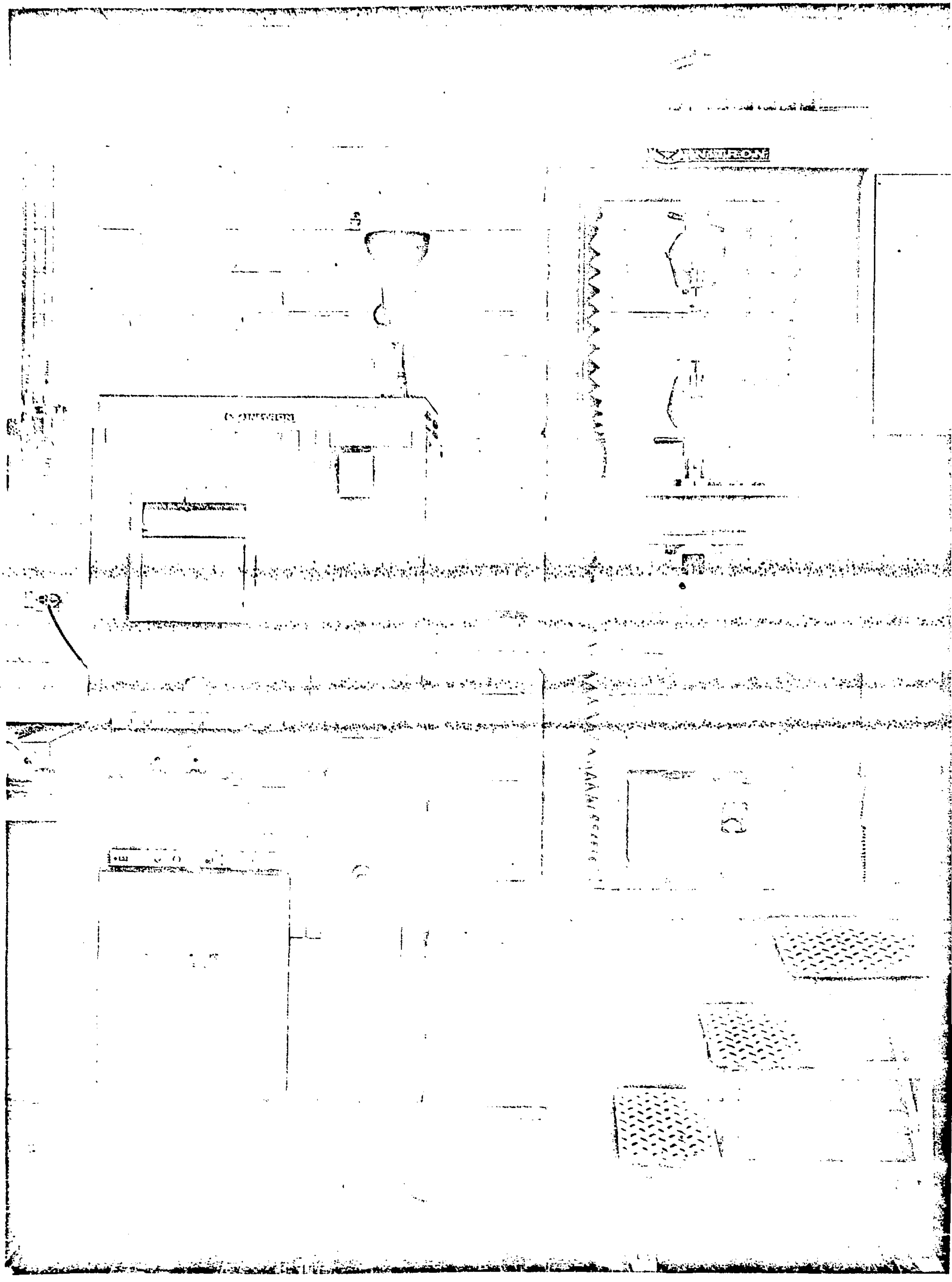

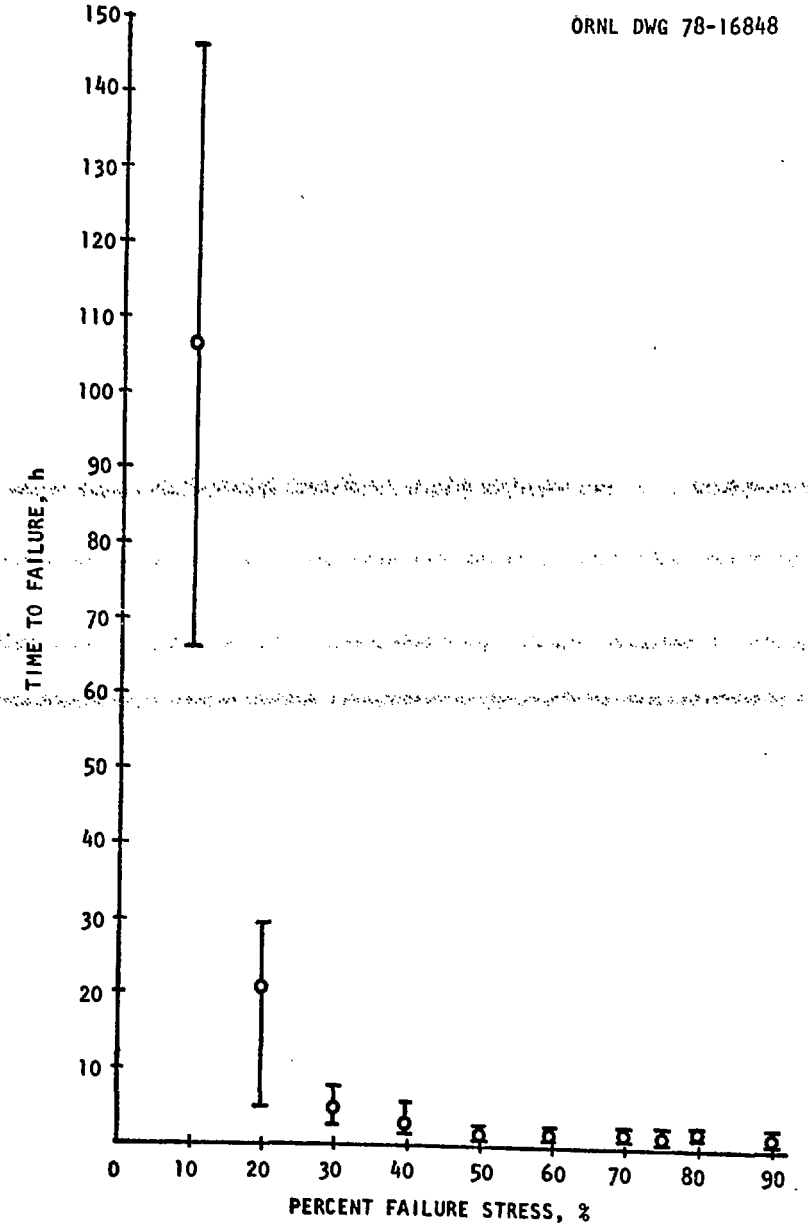
ORNL DWG 78-16848
TIME TO FAILURE, h
150
140
130
120
110
100
90
80
70
60
50
40
30
20
10
0
10
20
30
40
50
60
70
80
90
PERCENT FAILURE STRESS, %

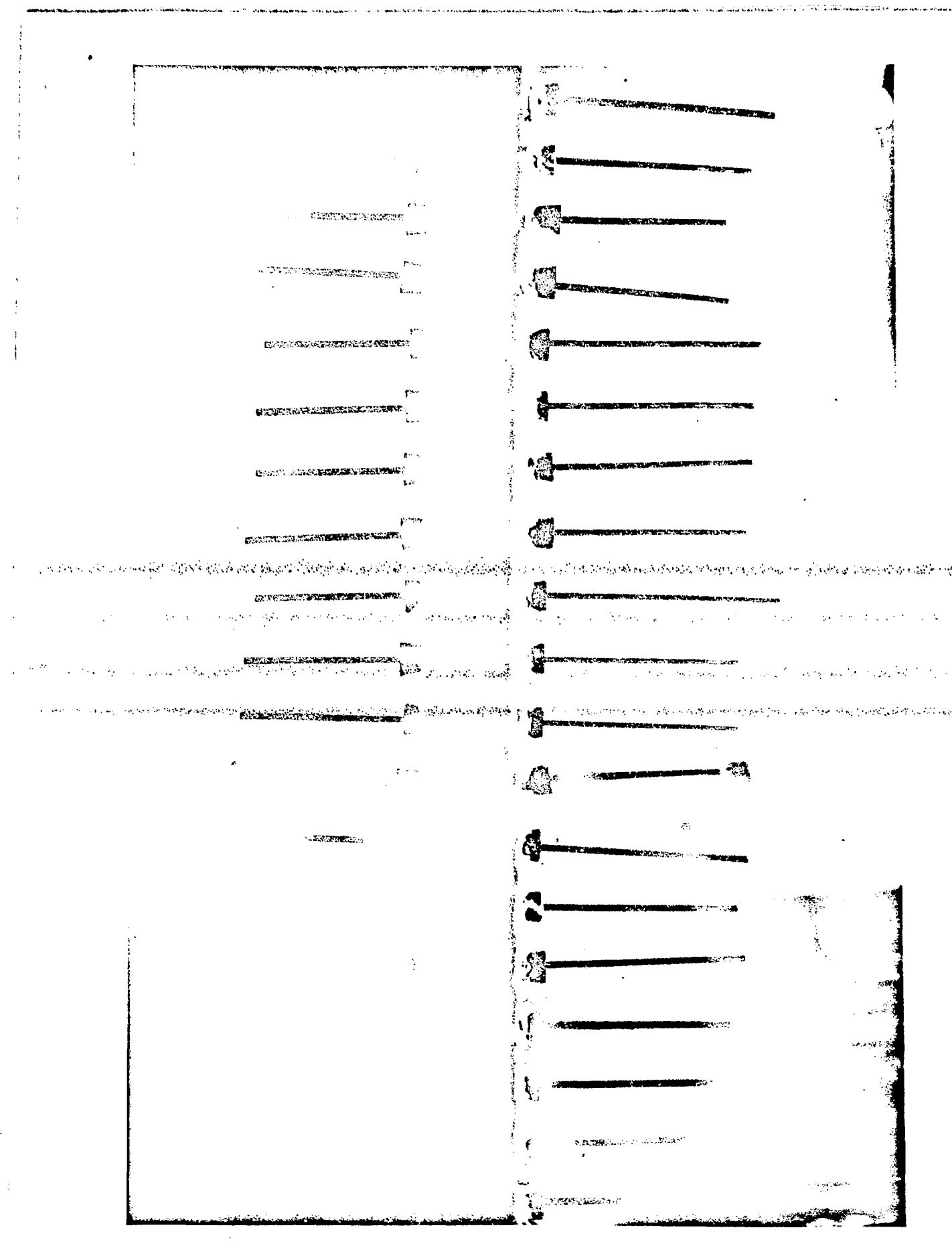

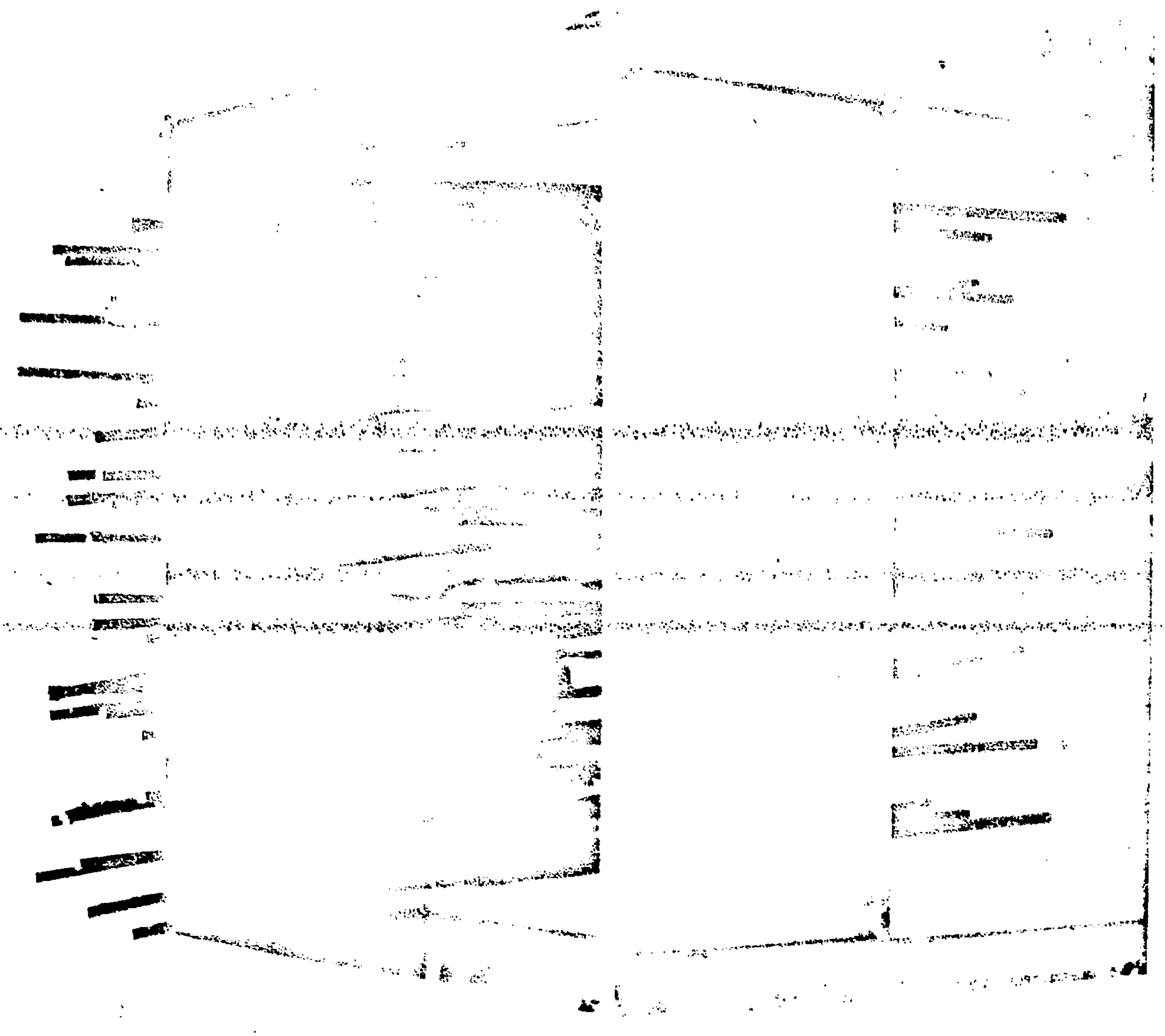

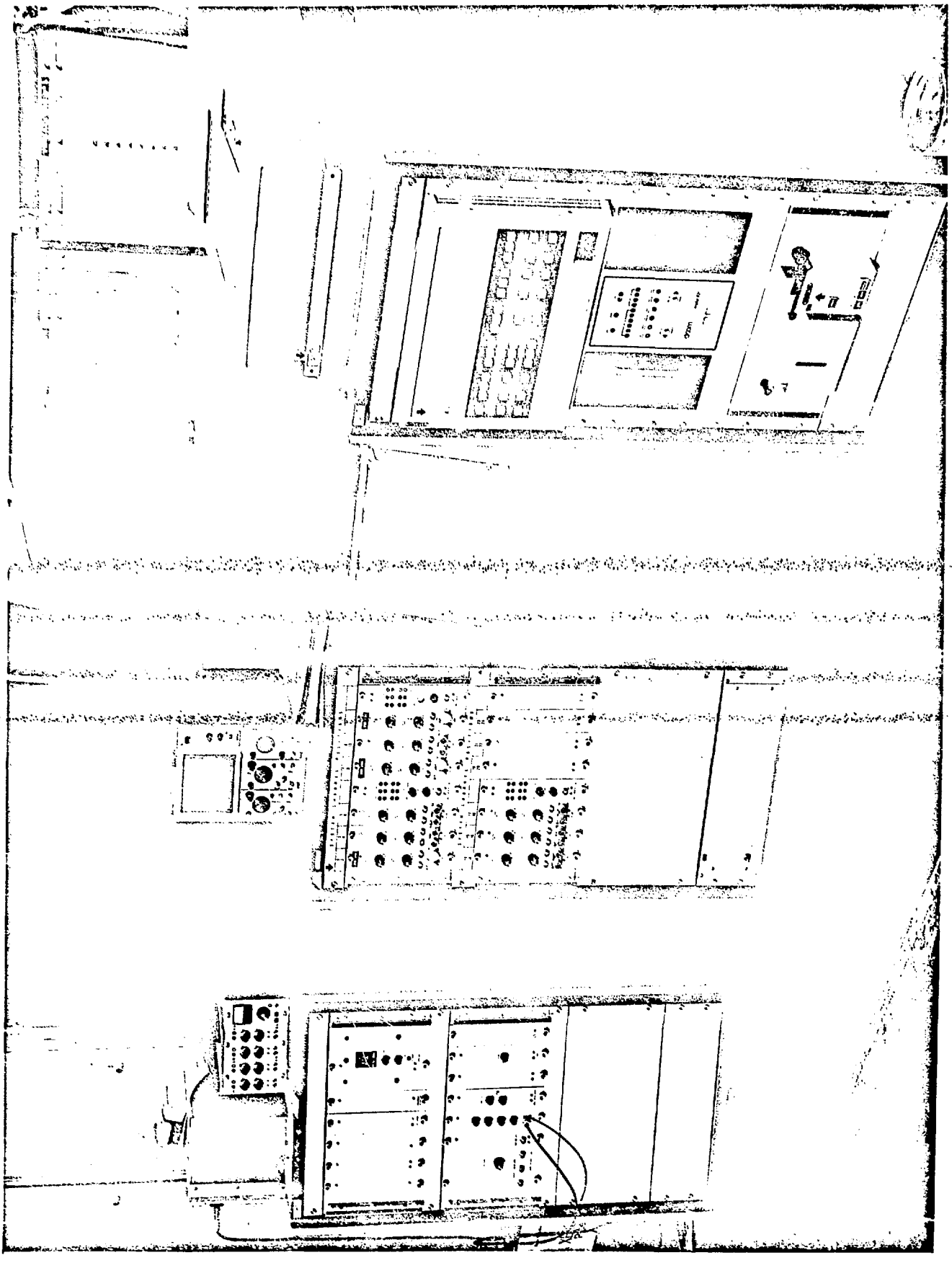

ORNL-DWG 78-6508

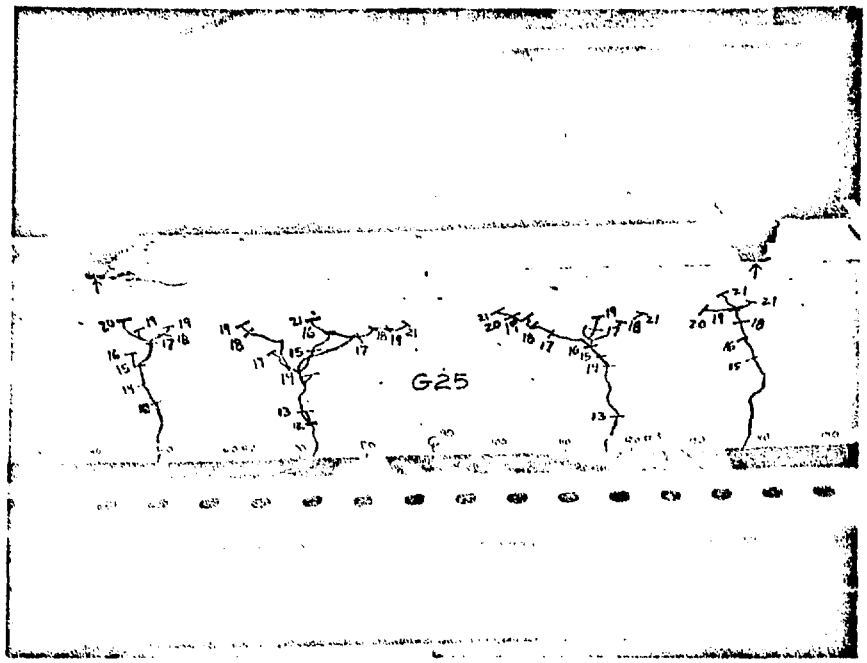

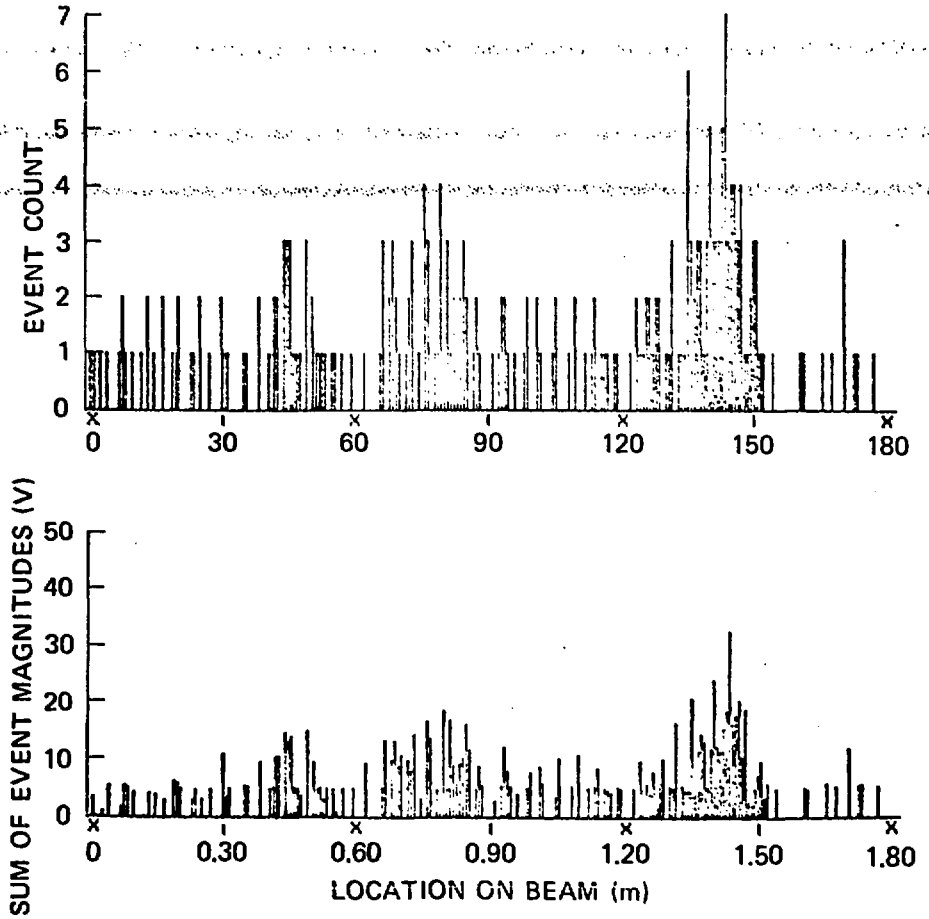

PRESTRESSED STRUCTURES EMPLOYING NONGROUTED TENDONS DEVELOP FEW LARGE CRACKS WHICH ARE DETECTABLE BY ACOUSTIC EMISSION.

ORNL DWG 78-8434

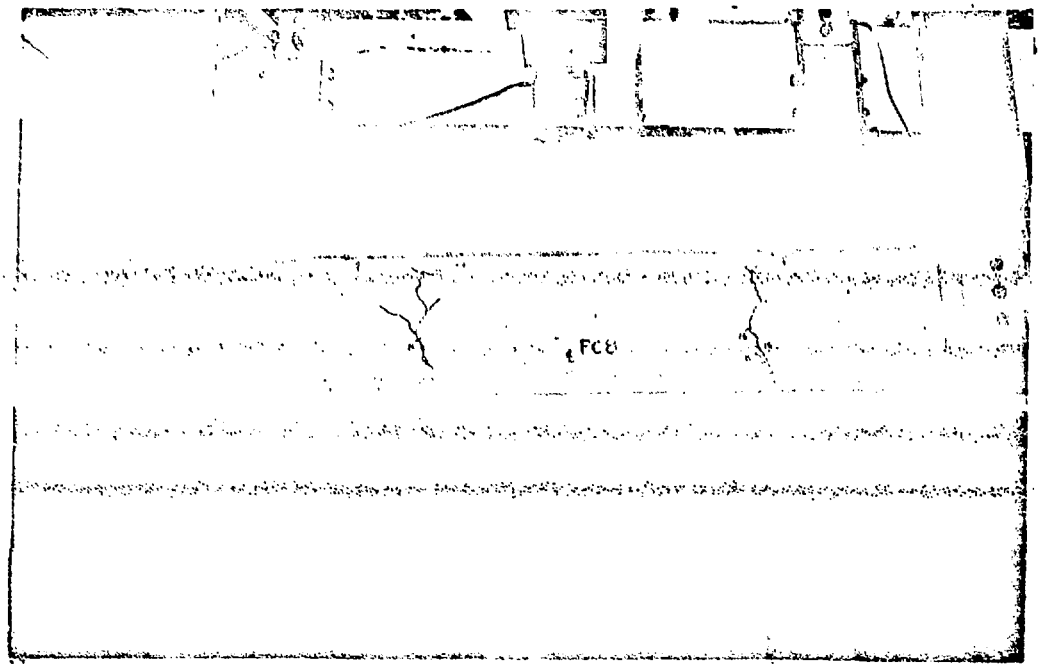

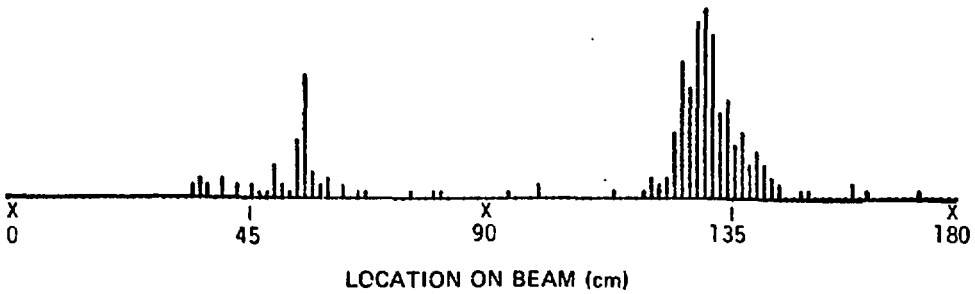

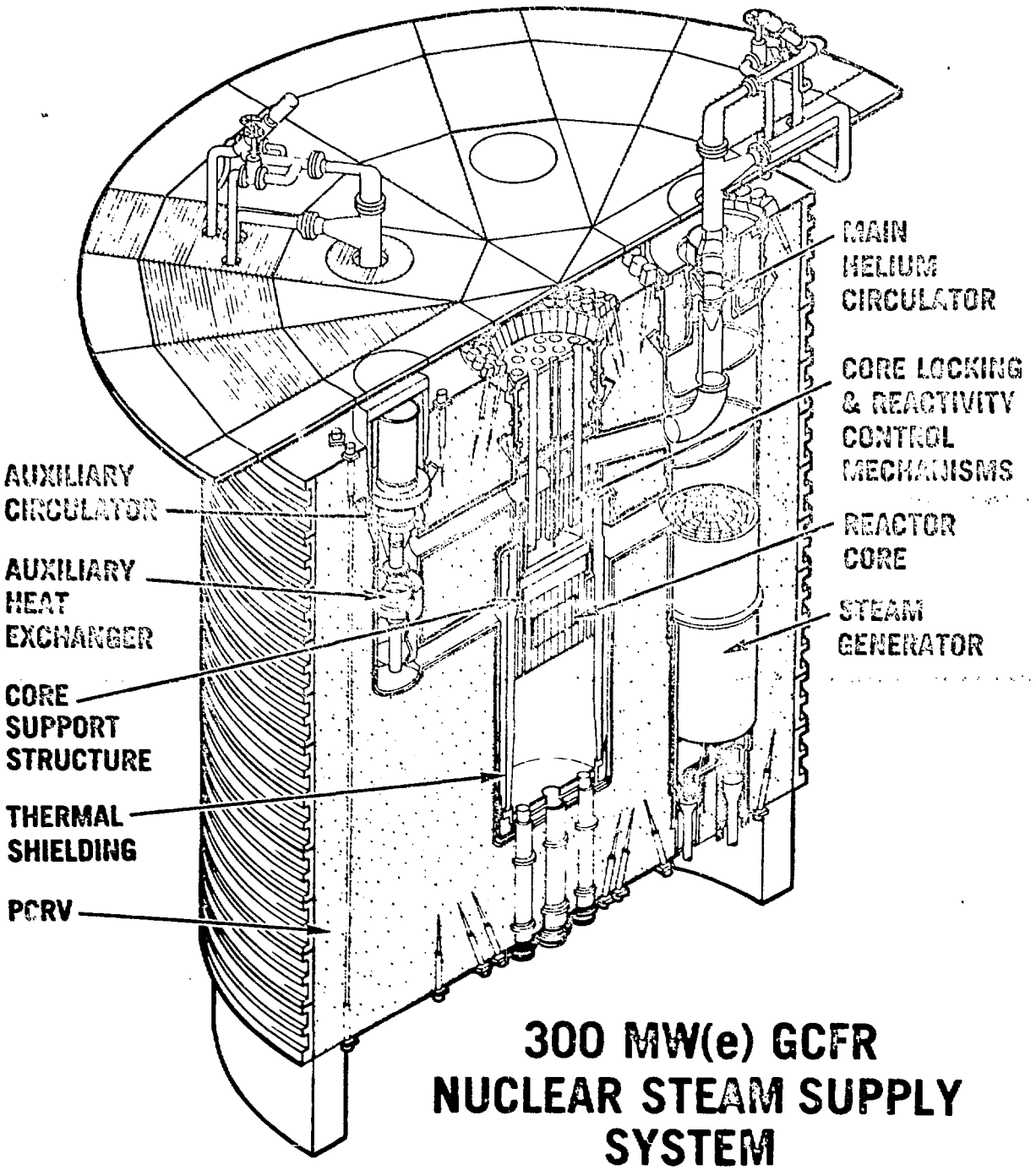

300 MW(e) GCFR NUCLEAR STEAM SUPPLY SYSTEM

ORNL-DWG 75-9729R

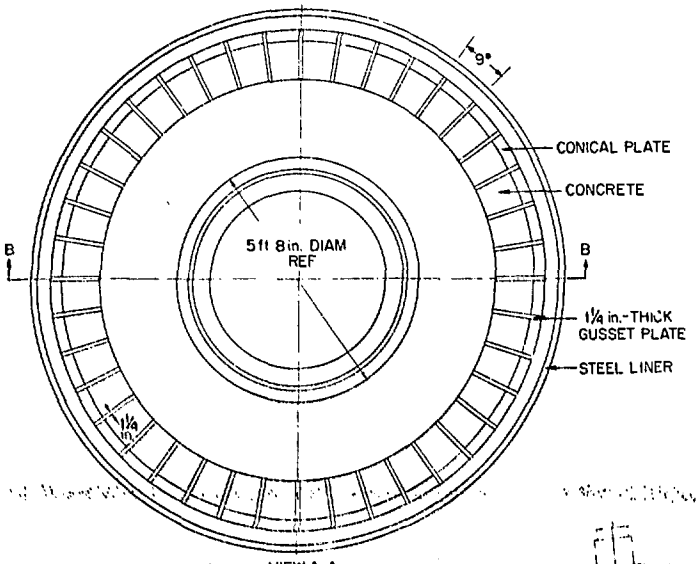

VIEW A-A

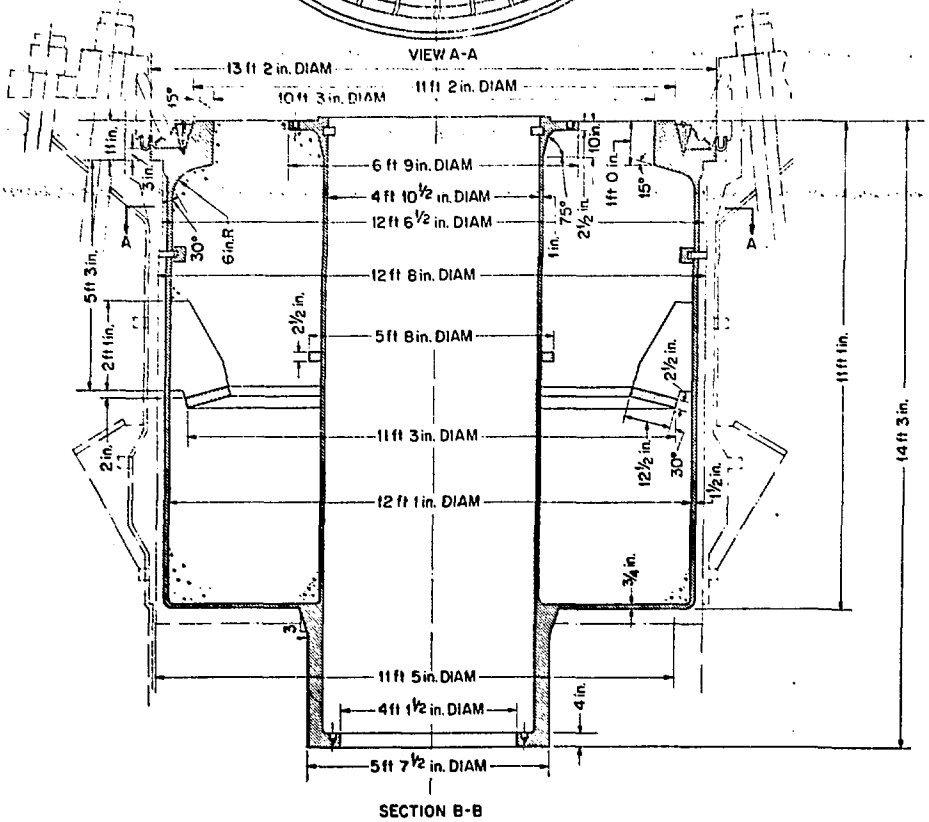

SECTION B-B

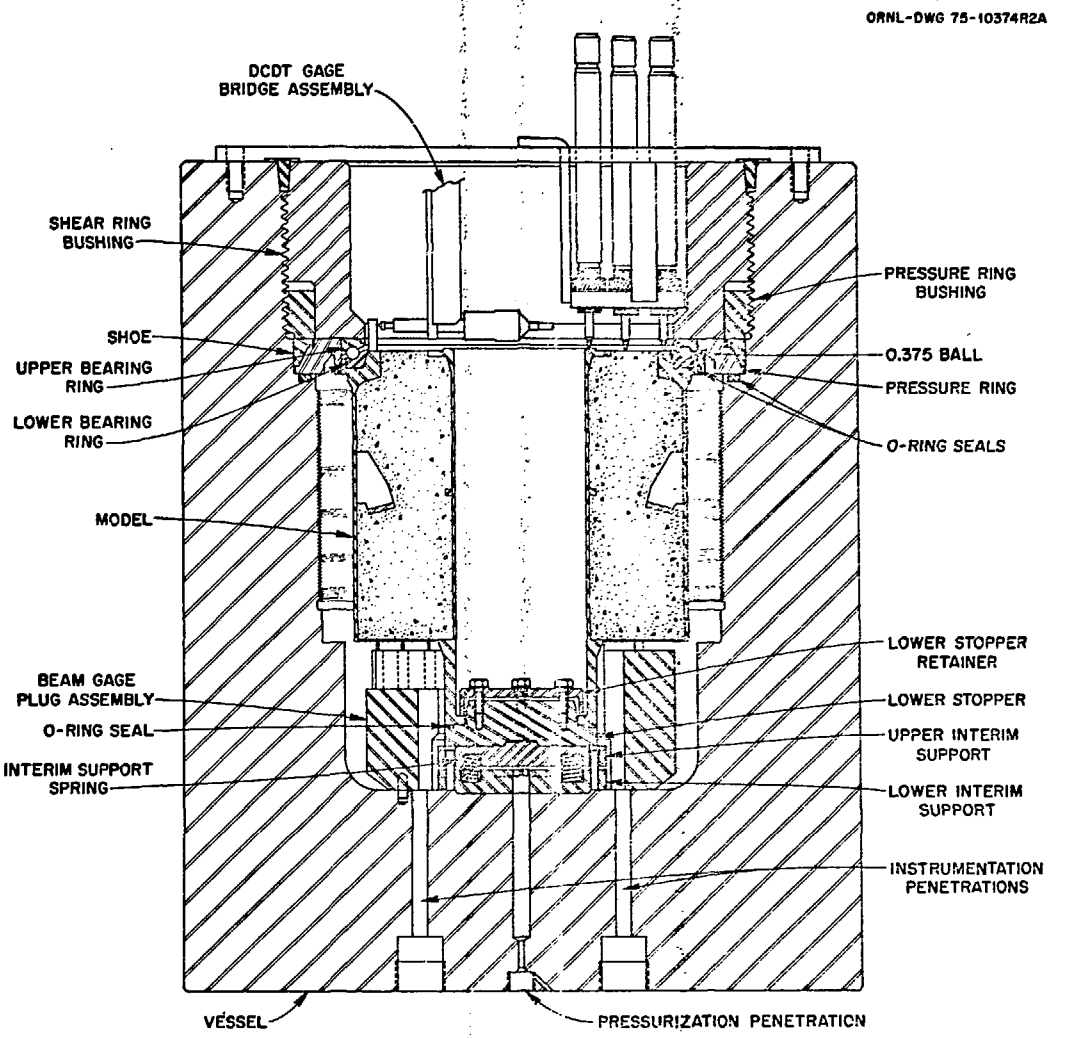
ORNL-DWG 75-10374R2A
DCDT GAGE BRIDGE ASSEMBLY
SHEAR RING BUSHING
SHOE
UPPER BEARING RING
LOWER BEARING RING
MODEL
BEAM GAGE PLUG ASSEMBLY
O-RING SEAL
INTERIM SUPPORT SPRING
VESSEL
PRESSURE RING BUSHING
0.375 BALL
PRESSURE RING
O-RING SEALS
LOWER STOPPER RETAINER
LOWER STOPPER
UPPER INTERIM SUPPORT
LOWER INTERIM SUPPORT
INSTRUMENTATION PENETRATIONS
PRESSURIZATION PENETRATION

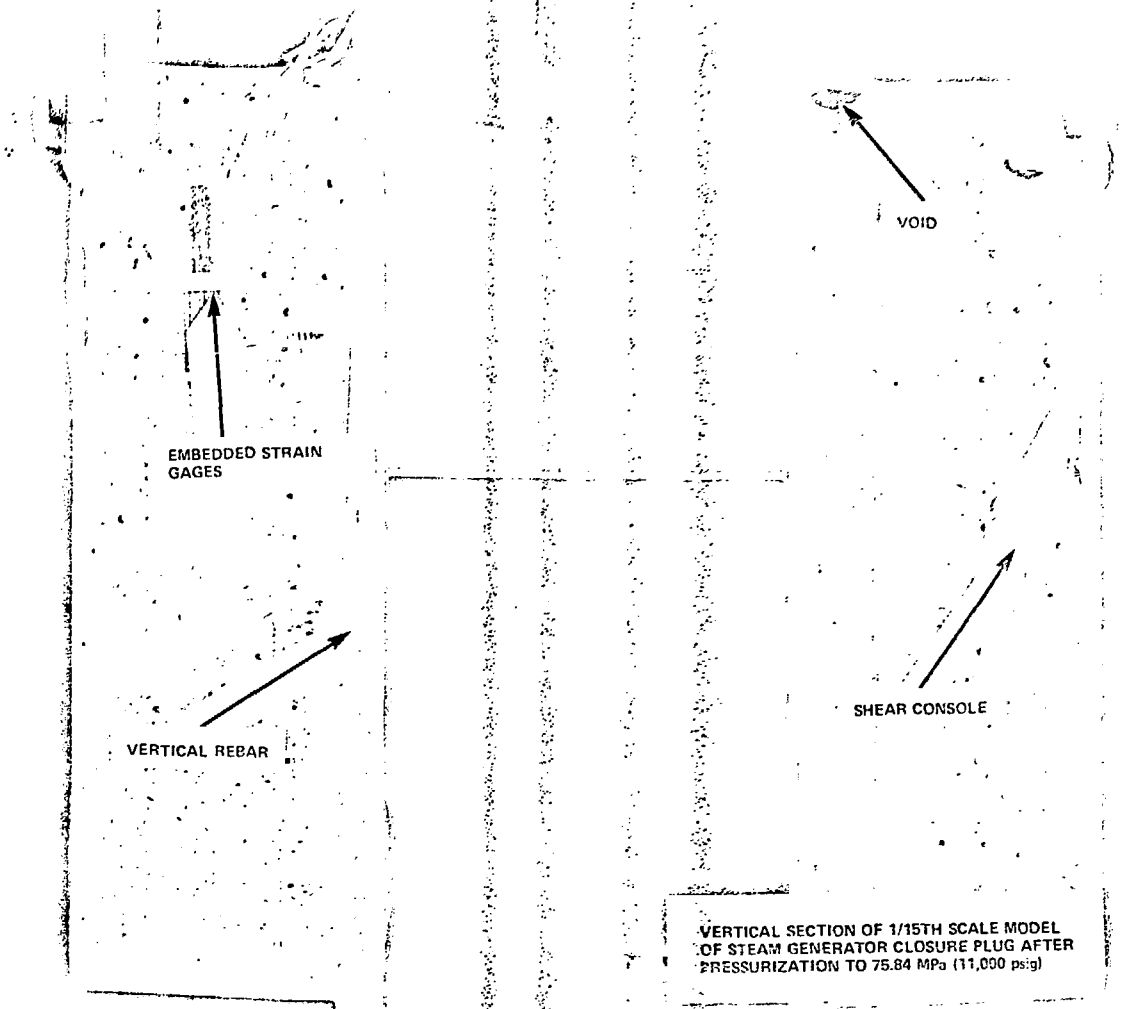

VERTICAL SECTION OF 1/15TH SCALE MODEL OF STEAM GENERATOR CLOSURE PLUG AFTER PRESSURIZATION TO 75.84 MPa (11,000 psig)